Probabilistic Engineering Mechanics 68 (2022) 103232

Contents lists available at ScienceDirect

Probabilistic Engineering Mechanics

journal homepage: www.elsevier.com/locate/probengmech

Probabilistic solution of a homogeneous linear second-order differential equation with randomized complex coefficients

A. Navarro-Quiles

Department of Statistics and Operational Research, Universitat de València, Dr. Moliner 50, 46100, Burjassot, Spain

ARTICLE INFO

Keywords:
Random complex differential equation
Probability density function
Random variable transformation method
Uncertainty quantification
Second-order differential equation
Simple harmonic oscillator

ABSTRACT

In this paper, an exact expression for the first probability density function of the solution stochastic process to a randomized homogeneous linear second-order complex differential equation is determined. To complete the probabilistic analysis, the first probability density functions of the real and complex contributions of the solution stochastic process are also calculated. To compute the densities, the random variable transformation method is applied under general hypothesis, all coefficients and initial conditions are absolutely continuous complex random variables. The capability of the theoretical results established is demonstrated by several numerical examples. Finally, we show the applicability of the method in engineering, by analysing the solution of a randomized simple harmonic oscillator, defined on the complex domain, and comparing our results with those obtained by using Monte Carlo simulations.

1. Introduction

Differential equations have been demonstrated to be an essential tool in Engineering. Differential equations permit to model numerous physical phenomenons and they are fundamental to analyse the behaviour of a given system of interest. In particular, second-order differential equations play a central role in the physical sciences. Many examples of the applicability of a second-order differential equations can be found in the literature, for instance, in mechanical vibration, electric circuits, classical mechanics and electrodynamics [1–3]. In the classical deterministic theory of differential equations, the coefficients, and the initial conditions considered to start the process, are usually fixed via experiments. Therefore, they contain a certain measurement error. This matter, along with the inherent complexity of the problems under study and some external factors that can affect to the system, make necessary to consider randomness in the formulation. There exist two main classes of differential equations with uncertainty, the stochastic differential equations (SDEs) and the random differential equations (RDEs). In the first case, differential equations are forced by an irregular stochastic process. A classical example of SDE is a differential equation perturbed by a term dependent on a white noise variable calculated as the derivate of the Wiener process or Brownian motion [4,5]. To solve a SDE we can use the so-called Itô calculus which is based on the application of the Itô lemma [5]. On the other hand, a RDE consists in a natural generalization of the deterministic counterpart [6–8]. That is, input parameters in the problem are considered random variables (RVs) or stochastic processes (SPs) rather than fixed constants or functions, respectively. The main advantage in dealing with RDEs is that we are able to assign a wide range of probabilistic distributions to the inputs, such as Gaussian, Gamma, Beta, Uniform, etc, . . . In addition, dependence among parameters can be considered. Thus, RDEs provide us flexibility to cope with real models.

In [9], the first probability density function (1-PDF) of the solution SP of a randomized homogeneous linear second-order differential equation is constructed considering that the input parameters, constant coefficients and initial conditions, are real RVs. On the other hand, differential equations and complex analysis have a significant role in modern engineering and physics and they have multiple applications in quantum mechanics, fluid mechanics, nuclear engineering and complex geometry [10–13]. It should be noted that recently, in 2017, some physicists gave a relation of the linear complex differential equations with constant coefficients and Schrödinger equations, see [14]. Then, given the importance of complex differential equations, the goal of this paper is to extend the analysis in [9] to the complex scenario. Then, in this work, a particular linear second-order RDE with complex coefficients is considered. In order to compute the 1-PDF of the solution SP of an homogeneous linear second-order differential equation with randomized complex coefficients we apply the Random Variable Transformation (RVT) method. This technique has been successfully applied in previous works [15–20], and it will allows us to find exact expressions for the 1-PDF of the solution SP.

The paper is organized as follows. For clarity's sake, in Section 2 classical probabilistic results about the computation of the 1-PDF are summarized. In particular, the RVT method in its multidimensional version is stated. In Section 3, we provide a complete probabilistic

E-mail address: ana.navarro@uv.es.

https://doi.org/10.1016/j.probengmech.2022.103232
Received 4 May 2021; Received in revised form 22 November 2021; Accepted 3 February 2022
Available online 10 February 2022
0266-8920/

description of a randomized homogeneous linear second-order complex differential equation. We compute the 1-PDF of the solution SP applying the RVT method, in different scenarios motivated by the deterministic theory. To complete Section 3, expressions for the 1-PDF of the real and complex components of the solution SP are also determined. The capability of the theoretical results established is shown in Section 4, where several numerical examples are exhibited. In addition, an application of the results achieved is addressed in Section 5. The 1-PDF of the response of a randomized simple harmonic oscillator defined on the complex domain, as well as both the real and complex contributions, is determined. In this case, comparisons with Monte Carlo simulations are done. Section 6 draws the conclusions and future work.

2. Preliminary concepts

In this section we introduce some preliminary concepts regarding the computation of the first PDF and how it can be used to obtain some interesting statistical quantities of a given SP. Let $\mathbf{x}(t,\omega)$ be the solution SP of a RDE. Note that, in this contribution we use bold letters to indicated that we are dealing with vectors. To solve a RDE means not only to compute its solution, a desirable goal is the computation of its main statistical functions, such as the mean and the variance. If it is possible, a more convenient objective is the determination of the 1-PDF, $f_1(\mathbf{x},t)$, that gives a full probabilistic description of the solution SP $\mathbf{x}(t,\omega)$ in every time instant t. From $f_1(\mathbf{x},t)$ we can calculate all one-dimensional moments

$$\mathbb{E}\left[\mathbf{x}(t,\omega)^k\right] = \int_{\mathbb{R}^n} \mathbf{x}^k f_1(\mathbf{x},t)\,\mathrm{d}\mathbf{x}, \quad k=1,2,\dots,$$

being $\mathbf{x}=(x_1,\dots,x_n)^\top \in \mathbb{R}^n$. In particular, the mean and the variance are defined by

$$\mu_{\mathbf{x}}(t) = \mathbb{E}\left[\mathbf{x}(t,\omega)\right], \quad \sigma^2_{\mathbf{x}}(t) = \mathbb{V}\left[\mathbf{x}(t,\omega)\right] = \mathbb{E}\left[\mathbf{x}(t,\omega)^2\right] - \mathbb{E}\left[\mathbf{x}(t,\omega)\right]^2. \tag{1}$$

Furthermore, the 1-PDF is useful to compute the probability the solution lies on a particular set of interest $\mathcal{B}\in\mathbb{R}^n$, for a given time instant $\hat{t}>0$ fixed,

$$\mathbb{P}\left[\{\omega\in\Omega \,:\, \mathbf{x}(\hat{t},\omega)\in\mathcal{B}\}\right] = \int_{\mathcal{B}} f_1(\mathbf{x},\hat{t})\,\mathrm{d}\mathbf{x}.$$

Notice that, fixed $\hat{t}>0$ and $\alpha\in(0,1)$, the 1-PDF also permits constructing confidence regions by determining $z\in\mathbb{R}$ such that

$$\int_{\mathbb{R}^n} (f_1(\mathbf{x},\hat{t}) - z)\,\mathrm{d}\mathbf{x} = 1-\alpha, \qquad f_1(\mathbf{x},\hat{t}) \ge z. \tag{2}$$

The confidence region is the $\mathbb{R}^{n-1}$-manifold defined by $f_1(\mathbf{x},\hat{t}) = z$. As indicated at the introduction, the RVT method its an useful tool to determine the distribution of a random vector from mapping another random vector with a known PDF. The multidimensional version of the RVT method is stated below, in Theorem 1.

Theorem 1 (*Random Variable Transformation Method, [6]*). *Let $\mathbf{u}(\omega) = (u_1(\omega),\dots,u_n(\omega))^\top$ and $\mathbf{v}(\omega) = (v_1(\omega),\dots,v_n(\omega))^\top$ be two n-dimensional absolutely continuous random vectors. Let $\mathbf{r}:\mathbb{R}^n\to\mathbb{R}^n$ be a one-to-one deterministic transformation of $\mathbf{u}$ into $\mathbf{v}$, i.e., $\mathbf{v}=\mathbf{r}(\mathbf{u})$. Assume that $\mathbf{r}$ is continuous in $\mathbf{u}$ and has continuous partial derivatives with respect to $\mathbf{u}$. Then, if $f_{\mathbf{u}}(\mathbf{u})$ denotes the joint PDF of vector $\mathbf{u}(\omega)$, and $\mathbf{s}=\mathbf{r}^{-1} = (s_1(v_1,\dots,v_n),\dots,s_n(v_1,\dots,v_n))^\top$ represents the inverse mapping of $\mathbf{r} = (r_1(u_1,\dots,u_n),\dots,r_n(u_1,\dots,u_n))^\top$, the joint PDF of vector $\mathbf{v}(\omega)$ is given by*

$$f_{\mathbf{v}}(\mathbf{v}) = f_{\mathbf{u}}(\mathbf{s}(\mathbf{v}))\left|J_n\right|,$$

where $|J_n|$ is the absolute value of the Jacobian, which is defined by

$$J_n = \det\left(\frac{\partial \mathbf{s}^\top}{\partial \mathbf{v}}\right) = \det\begin{pmatrix} \dfrac{\partial s_1(v_1,\dots,v_n)}{\partial v_1} & \cdots & \dfrac{\partial s_n(v_1,\dots,v_n)}{\partial v_1} \\ \vdots & \ddots & \vdots \\ \dfrac{\partial s_1(v_1,\dots,v_n)}{\partial v_n} & \cdots & \dfrac{\partial s_n(v_1,\dots,v_n)}{\partial v_n} \end{pmatrix}.$$

3. Probabilistic solution of the solution SP

Let us consider the randomized homogeneous linear second-order complex differential equation

$$\ddot{x}(t,\omega) - d(\omega)x(t,\omega) = 0, \quad t>0, \tag{3}$$

with initial conditions

$$x(0,\omega) = a(\omega), \qquad \dot{x}(0,\omega) = b(\omega). \tag{4}$$

Remark 1. Note that in the subsequent development a complete randomized homogeneous linear second-order complex differential equation of the form

$$\ddot{x}(t,\omega) + p(\omega)\dot{x}(t,\omega) + q(\omega)x(t,\omega) = 0, \quad t>0,$$

can be considered. Given the complexity of the notation and calculations, a reduce version is treated in this paper. We consider the RDE (3) because of its applicability, for example in mechanical vibrations when considering unforced and undamped vibrations [1]. All computations can be reproduced considering the complete differential equation.

In the initial value problem (IVP) (3)–(4), input parameters $d(\omega)$, $a(\omega)$ and $b(\omega)$ are assumed to be dependent absolutely continuous complex RVs defined on a common complete probability space $(\Omega,\mathcal{F},\mathbb{P})$. Let us recall that a complex RV $z(\omega)$ is defined as a RV of the form

$$z(\omega) = z_R(\omega) + \mathrm{i}\, z_C(\omega),$$

where the real and the complex parts, $z_R(\omega)$ and $z_C(\omega)$, are real RVs, and i is the well-known imaginary unit, defined as $\mathrm{i}^2=-1$. The statistical information and properties of the complex RV $z(\omega)$ are determined by the joint PDF of the random vector $(z_R(\omega), z_C(\omega))^\top$, $f_{RC}(z_R,z_C)$, provided that it exists. For more information about complex RVs see for example Refs. [21–24] and therein. In order to apply RVT method, we consider that the joint PDF of the complex random vector $(d(\omega),a(\omega),b(\omega))^\top$ is known and it is denoted by $f_0(d_R,d_C,a_R,a_C,b_R,b_C)$. Then, for the sake of generality, we are assuming dependence between the complex RVs. In case of independent RVs we can apply that the joint PDF is the product of the marginals, that is

$$f_0(d_R,d_C,a_R,a_C,b_R,b_C) = f_d(d_R,d_C)f_a(a_R,a_C)f_b(b_R,b_C)$$

In addition, the real and complex components of a complex RV can also be independent. In this case, the joint PDF of the complex RV turns out to be the product of the PDF of the real component and the PDF of the complex component.

3.1. Computing the 1-PDF of the solution SP $x(t,\omega)$

As it has been indicated at the introduction, a RDE is a natural generalization of the deterministic counterpart. In this manner, firstly we shall find a closed expression for the solution of the deterministic IVP

$$\begin{cases} \ddot{x}(t) - d\,x(t) = 0, & t>0, \\ x(0)=a, & \dot{x}(0)=b, \end{cases} \tag{5}$$

where d,a,b are complex numbers. From the classical deterministic theory of differential equations, the solution of the deterministic differential equation given in (5) is

$$x(t) = E\,\mathrm{e}^{r_1 t} + F\,\mathrm{e}^{r_2 t},$$

being r_1 and r_2 the roots of the associated characteristic equation, $r^2 - d = 0$, and E and F constants determined from the initial conditions. First, we calculate the roots of the characteristic equation. In IVP (5) we are considering complex parameters, thus we must calculate the roots of a complex number, i.e., $r=\sqrt{d}$, with $d=d_R+\mathrm{i}\,d_C$. It is easy to prove that the roots of a complex number $d=d_R+\mathrm{i}\,d_C$ are:

- Scenario 1. If $d_C > 0$:

$$r_1 = \sqrt{\frac{d_R + \sqrt{d_R^2 + d_C^2}}{2}} + \mathrm{i}\sqrt{\frac{-d_R + \sqrt{d_R^2 + d_C^2}}{2}}, \qquad r_2 = -r_1.$$

- Scenario 2. If $d_C < 0$:

$$r_1 = \sqrt{\frac{d_R + \sqrt{d_R^2 + d_C^2}}{2}} - \mathrm{i}\sqrt{\frac{-d_R + \sqrt{d_R^2 + d_C^2}}{2}}, \qquad r_2 = -r_1.$$

- Scenario 3. If $d_C = 0$, then $d = d_R$ is a real number and we have to distinguish the following cases:
  - If $d_R > 0$, then $r_1 = +\sqrt{d_R}$ and $r_2 = -r_1$.
  - If $d_R < 0$, then $r_1 = +\mathrm{i}\sqrt{-d_R}$ and $r_2 = -r_1$.
  - If $d_R = 0$, then $r_1 = r_2 = 0$.

3.1.1. Computing the 1-PDF in the first and second scenarios

From the initial conditions, we calculate the constants E and F by solving the linear system

$$\begin{aligned} a &= x(0) = E + F, \\ b &= \dot{x}(0) = Er_1 + Fr_2 = r_1(E - F), \end{aligned}$$

obtaining

$$E = \frac{a}{2} + \frac{b}{2r_1}, \qquad F = \frac{a}{2} - \frac{b}{2r_1}.$$

Then, the solution of the deterministic IVP (5) is

$$x(t) = \left(\frac{a}{2} + \frac{b}{2r_1}\right)\mathrm{e}^{r_1 t} + \left(\frac{a}{2} - \frac{b}{2r_1}\right)\mathrm{e}^{-r_1 t}, \tag{6}$$

where $r_1 := r_1(d_R, d_C) \in \mathbb{C}$ is the principal root defined above in each scenario (notice that, in these scenarios, r_1 and r_2 are not simultaneously zero), and its expression depends on the sign of d_C. As it has been previously indicated, in the random scenario, for each t fixed, the distribution of the complex RV $x(t,\omega)$ is determined by the joint distribution of the real and the complex components. Therefore, expression (6) should be written with a distinction between the real and the complex components, in order to find the transformation to apply the RVT method. Let $a = a_R + \mathrm{i}\, a_C$, $b = b_R + \mathrm{i}\, b_C$ and $r_1 = r_{1R} + \mathrm{i}\, r_{1C}$, from the properties of complex numbers, in particular de Euler's Formula, the real and complex components of $x(t)$ are

$$\begin{aligned} x_R(t) = \frac{\mathrm{e}^{r_{1R}t}}{2}\Bigg(&\left(a_R + \frac{b_R r_{1R} + b_C r_{1C}}{r_{1R}^2 + r_{1C}^2}\right)\cos \\ &- \left(a_C - \frac{b_R r_{1C} - b_C r_{1R}}{r_{1R}^2 + r_{1C}^2}\right)\sin(r_{1C}t)\Bigg) \\ &+ \frac{\mathrm{e}^{-r_{1R}t}}{2}\Bigg(\left(a_R - \frac{b_R r_{1R} + b_C r_{1C}}{r_{1R}^2 + r_{1C}^2}\right)\cos(r_{1C}t) \\ &+ \left(a_C + \frac{b_R r_{1C} - b_C r_{1R}}{r_{1R}^2 + r_{1C}^2}\right)\sin(r_{1C}t)\Bigg), \end{aligned}$$

$$\begin{aligned} x_C(t) = \frac{\mathrm{e}^{r_{1R}t}}{2}\Bigg(&\left(a_R + \frac{b_R r_{1R} + b_C r_{1C}}{r_{1R}^2 + r_{1C}^2}\right)\sin(r_{1C}t) \\ &+ \left(a_C - \frac{b_R r_{1C} - b_C r_{1R}}{r_{1R}^2 + r_{1C}^2}\right)\cos(r_{1C}t)\Bigg) \\ &+ \frac{\mathrm{e}^{-r_{1R}t}}{2}\Bigg(-\left(a_R - \frac{b_R r_{1R} + b_C r_{1C}}{r_{1R}^2 + r_{1C}^2}\right)\sin \\ &+ \left(a_C + \frac{b_R r_{1C} - b_C r_{1R}}{r_{1R}^2 + r_{1C}^2}\right)\cos(r_{1C}t)\Bigg). \end{aligned}$$

After some algebra the expressions of the real and complex contribution can be written in a more compact formulation:

$$\begin{aligned} x_R(t; a_R, a_C, \mathbf{y}) &= \quad a_R g_1(t;\mathbf{y}) + a_C g_2(t;\mathbf{y}) + g_3(t;\mathbf{y}), \\ x_C(t; a_R, a_C, \mathbf{y}) &= -a_R g_2(t;\mathbf{y}) + a_C g_1(t;\mathbf{y}) + g_4(t;\mathbf{y}), \end{aligned}$$

being

$$\begin{aligned} g_1(t;\mathbf{y}) &:= g_1(t; b_R, b_C, d_R, d_C) = \cos(r_{1C}t)\cosh(r_{1R}t), \\ g_2(t;\mathbf{y}) &:= g_2(t; b_R, b_C, d_R, d_C) = -\sin(r_{1C}t)\sinh(r_{1R}t), \\ g_3(t;\mathbf{y}) &:= g_3(t; b_R, b_C, d_R, d_C) = \cos(r_{1C}t)\sinh(r_{1R}t)\frac{b_R r_{1R} + b_C r_{1C}}{r_{1R}^2 + r_{1C}^2} \\ &\qquad + \sin(r_{1C}t)\cosh(r_{1R}t)\frac{b_R r_{1C} - b_C r_{1R}}{r_{1R}^2 + r_{1C}^2}, \\ g_4(t;\mathbf{y}) &:= g_4(t; b_R, b_C, d_R, d_C) = -\cos(r_{1C}t)\sinh(r_{1R}t)\frac{b_R r_{1C} - b_C r_{1R}}{r_{1R}^2 + r_{1C}^2} \\ &\qquad + \sin(r_{1C}t)\cosh(r_{1R}t)\frac{b_R r_{1R} + b_C r_{1C}}{r_{1R}^2 + r_{1C}^2}, \end{aligned} \tag{7}$$

where $\mathbf{y} = (b_R, b_C, d_R, d_C)$. Notice that, as it will be shown later, this reformulation of the solution will be useful in the application of the RVT method. So, the solution SP of the random IVP (3)–(4) is derived from the deterministic solution,

$$x(t,\omega) = x_R(t,\omega) + \mathrm{i}\, x_C(t,\omega),$$

where $x_R(t,\omega)$ and $x_C(t,\omega)$ are given by

$$\begin{aligned} x_R(t,\omega) &:= x_R(t; a_R(\omega), a_C(\omega), \mathbf{y}(\omega)) \\ &= a_R(\omega)g_1(t;\mathbf{y}(\omega)) + a_C(\omega)g_2(t;\mathbf{y}(\omega)) + g_3(t;\mathbf{y}(\omega)), \end{aligned} \tag{8}$$

$$\begin{aligned} x_C(t,\omega) &:= x_C(t; a_R(\omega), a_C(\omega), \mathbf{y}(\omega)) \\ &= -a_R(\omega)g_2(t;\mathbf{y}(\omega)) + a_C(\omega)g_1(t;\mathbf{y}(\omega)) + g_4(t;\mathbf{y}(\omega)), \end{aligned} \tag{9}$$

being the stochastic processes $g_i(t;\mathbf{y}(\omega))$, $i \in \{1,2,3,4\}$, obtained as a randomization of the corresponding deterministic counterpart defined in (7). In Eqs. (8) and (9) both SPs $x_R(t,\omega)$ and $x_C(t,\omega)$ depend upon RVs $a_R(\omega)$, $a_C(\omega)$, $b_R(\omega)$, $b_C(\omega)$, $r_{1R}(\omega)$ and $r_{1C}(\omega)$. At the same time RVs $r_{1R}(\omega)$ and $r_{1C}(\omega)$ are calculated from $d_R(\omega)$ and $d_C(\omega)$, as previously indicated. Given a fixed time instant $t > 0$, we apply the RVT method to compute the PDF of the random vector $\mathbf{v}(\omega) = \left(v_1(\omega), v_2(\omega), v_3(\omega), v_4(\omega), v_5(\omega), v_6(\omega)\right)^\top$ in terms of the known PDF of the input random parameters $\mathbf{u}(\omega) = (a_R(\omega), a_C(\omega), b_R(\omega), b_C(\omega), d_R(\omega), d_C(\omega))^\top$, $f_0(\mathbf{u}) = f_0(a_R, a_C, b_R, b_C, d_R, d_C)$. We define the mapping $\mathbf{r} : \mathbb{R}^6 \to \mathbb{R}^6$

$$\begin{aligned} v_1 &= r_1(\mathbf{u}) = x_R(t) = a_R g_1(t;\mathbf{y}) + a_C g_2(t;\mathbf{y}) + g_3(t;\mathbf{y}), \\ v_2 &= r_2(\mathbf{u}) = x_C(t) = -a_R g_2(t;\mathbf{y}) + a_C g_1(t;\mathbf{y}) + g_4(t;\mathbf{y}), \\ \hat{\mathbf{v}} &= \hat{\mathbf{r}}(\mathbf{u}) = \mathbf{y}, \end{aligned}$$

where $\hat{\mathbf{v}} = (v_3, v_4, v_5, v_6)$, $\hat{\mathbf{r}} = (r_3, r_4, r_5, r_6)$ and $\mathbf{y} = (b_R, b_C, d_R, d_C)$. The inverse of the mapping $\mathbf{r}$, $\mathbf{s} : \mathbb{R}^6 \to \mathbb{R}^6$, is

$$\begin{aligned} a_R &= s_1(\mathbf{v}) = \frac{(v_1 - g_3(y;\hat{\mathbf{v}}))g_1(y;\hat{\mathbf{v}}) - (v_2 - g_4(y;\hat{\mathbf{v}}))g_2(y;\hat{\mathbf{v}})}{g_1(y;\hat{\mathbf{v}})^2 + g_2(y;\hat{\mathbf{v}})^2}, \\ a_C &= s_2(\mathbf{v}) = \frac{(v_2 - g_4(y;\hat{\mathbf{v}}))g_1(y;\hat{\mathbf{v}}) + (v_1 - g_3(y;\hat{\mathbf{v}}))g_2(y;\hat{\mathbf{v}})}{g_1(y;\hat{\mathbf{v}})^2 + g_2(y;\hat{\mathbf{v}})^2}, \\ \mathbf{y} &= \hat{\mathbf{s}}(\mathbf{v}) = \hat{\mathbf{v}}. \end{aligned}$$

where $\hat{\mathbf{s}} = (s_3, s_4, s_5, s_6)$ is the inverse mapping of $\hat{\mathbf{r}} = (r_3, r_4, r_5, r_6)$. The Jacobian of mapping $\mathbf{s}$ is

$$J = \frac{1}{g_1(y;\hat{\mathbf{v}})^2 + g_2(y;\hat{\mathbf{v}})^2} = \frac{2}{\cos(2r_{1C}t) + \cosh(2r_{1R}t)} > 0.$$

The Jacobian is strictly positive because of the hyperbolic cosine function is greater than or equal to 1. In addition, $\cosh(2r_{1R}t) = 1$ if $t = 0$ or $r_{1R} = 0$. In this case, the time instant t considered is positive and we are dealing with the first and second scenarios, therefore r_{1R} is also nonzero. Then, applying Theorem 1, we obtain the joint PDF of the random vector $\mathbf{v}(\omega)$ in terms of the PDF of the random input parameters

$$f_{\mathbf{v}}(\mathbf{v}) = f_0(s_1(\mathbf{v}), s_2(\mathbf{v}), v_3, v_4, v_5, v_6)\frac{2}{\cos(2r_{1C}t) + \cosh(2r_{1R}t)}. \tag{10}$$

The distribution of the solution SP of the random IVP (3)–(4) is determined by the joint PDF of the random vector $(v_1(\omega), v_2(\omega))^\top = (x_R(t,\omega), x_C(\omega))^\top$. In order to compute it, we marginalize expression (10) with respect to $\hat{\mathbf{v}}(\omega) = (b_R(\omega), b_C(\omega), d_R(\omega), d_C(\omega))^\top = \mathbf{y}(\omega)^\top$. Then, marginalizing and taking $t > 0$ arbitrary the 1-PDF of the solution SP $x(t,\omega)$ is

$$f_1(x_R, x_C, t) = \int_{\mathbb{R}^4} f_0\left(s_1(x_R, x_C, \mathbf{y}), s_2(x_R, x_C, \mathbf{y}), \mathbf{y}\right) \times \frac{2}{\cos(2r_{1C}(d_R, d_C)t) + \cosh(2r_{1R}(d_R, d_C)t)} \mathrm{d}\mathbf{y}, \tag{11}$$

being r_{1R} and r_{1C} the real and complex contributions, respectively, of the principal root r_1 defined in Section 3.1. Note that, the principal root of the characteristic equation, $r_1(\omega)$, depends on the sign of $d_C(\omega)$, for all $\omega \in \Omega$. Therefore, if the domain of the RV $d_C(\omega)$ is positive we consider the first scenario. Then, the 1-PDF is

$$f_1^+(x_R, x_C, t) = \int_{\mathbb{R}^+} \int_{\mathbb{R}^3} f_0\left(s_1(x_R, x_C, \mathbf{y}), s_2(x_R, x_C, \mathbf{y}), \mathbf{y}\right) \times \frac{2}{\cos(2r_{1C}(d_R, d_C)t) + \cosh(2r_{1R}(d_R, d_C)t)} \mathrm{d}b_R\, \mathrm{d}b_C\, \mathrm{d}d_R\, \mathrm{d}d_C, \tag{12}$$

where $r_{1R}(d_R, d_C) = \sqrt{\frac{d_R + \sqrt{d_R^2 + d_C^2}}{2}}$ and $r_{1C}(d_R, d_C) = \sqrt{\frac{-d_R + \sqrt{d_R^2 + d_C^2}}{2}}$. If the domain of $d_C(\omega)$ is negative we must deal with the second scenario. Thus, the expression of the 1-PDF is

$$f_1^-(x_R, x_C, t) = \int_{\mathbb{R}^-} \int_{\mathbb{R}^3} f_0\left(s_1(x_R, x_C, \mathbf{y}), s_2(x_R, x_C, \mathbf{y}), \mathbf{y}\right) \times \frac{2}{\cos(2r_{1C}(d_R, d_C)t) + \cosh(2r_{1R}(d_R, d_C)t)} \mathrm{d}b_R\, \mathrm{d}b_C\, \mathrm{d}d_R\, \mathrm{d}d_C, \tag{13}$$

where $r_{1R}(d_R, d_C) = \sqrt{\frac{d_R + \sqrt{d_R^2 + d_C^2}}{2}}$ and $r_{1C}(d_R, d_C) = -\sqrt{\frac{-d_R + \sqrt{d_R^2 + d_C^2}}{2}}$. Finally, if the domain has both negative and positive values, the 1-PDF expressed in (11) must be split into two integrals, considering for the positive values the roots of the first scenario and for the negative the roots of the second, that is

$$f_1(x_R, x_C, t) = f_1^+(x_R, x_C, t) + f_1^-(x_R, x_C, t).$$

3.1.2. Computing the 1-PDF in the third scenario

Now, we obtain expressions for the 1-PDF in the third scenario. First we study the case where the coefficient $d(\omega)$ is a real RV, i.e., $d(\omega) = d_R(\omega)$. In the second part of this subsection we will assume that the coefficient d in (5) is zero.

Let us start considering that $\mathbb{P}\left[\omega \in \Omega \,:\, d_R(\omega) < 0\right] = 1$. Given a fixed time $t > 0$, the mapping $\mathbf{r} : \mathbb{R}^5 \to \mathbb{R}^5$ is

$$\begin{aligned}
v_1 &= r_1(\mathbf{u}) = x_R(t) = a_R \cos(\sqrt{-d_R}t) + \frac{b_R}{\sqrt{-d_R}} \sin(\sqrt{-d_R}t),\\
v_2 &= r_2(\mathbf{u}) = x_C(t) = a_C \cos(\sqrt{-d_R}t) + \frac{b_C}{\sqrt{-d_R}} \sin(\sqrt{-d_R}t),\\
v_3 &= r_3(\mathbf{u}) = b_R,\\
v_4 &= r_4(\mathbf{u}) = b_C,\\
v_5 &= r_5(\mathbf{u}) = d_R,
\end{aligned}$$

where $\mathbf{u} = (a_R, a_C, b_R, b_C, d_R)^\top$ and $\mathbf{v} = (v_1, v_2, \ldots, v_5)^\top$. The inverse mapping $\mathbf{s} : \mathbb{R}^5 \to \mathbb{R}^5$ and its Jacobian are given by

$$\begin{aligned}
a_R &= s_1(\mathbf{v}) = \frac{\sec(\sqrt{-v_5}t)}{\sqrt{-v_5}} \left(\sqrt{-v_5}v_1 - v_3 \sin(\sqrt{-v_5}t)\right),\\
a_C &= s_2(\mathbf{v}) = \frac{\sec(\sqrt{-v_5}t)}{\sqrt{-v_5}} \left(\sqrt{-v_5}v_2 - v_4 \sin(\sqrt{-v_5}t)\right),\\
b_R &= s_3(\mathbf{v}) = v_3,\\
b_C &= s_4(\mathbf{v}) = v_4,\\
d_R &= s_5(\mathbf{v}) = v_5,
\end{aligned}$$

$$J = \sec(\sqrt{-v_5}t).$$

Then, applying the RVT method the joint PDF of the random vector $\mathbf{v}(\omega)$ is

$$f_{\mathbf{v}}(\mathbf{v}) = f_0\left(s_1(\mathbf{v}), s_2(\mathbf{v}), v_3, v_4, v_5\right) \left|\sec(\sqrt{-v_5}t)\right|,$$

where $f_0(a_R, a_C, b_R, b_C, d_R)$ the joint PDF of the random input parameters, i.e., the PDF of the random vector $(a_R(\omega), a_C(\omega), b_R(\omega), b_C(\omega), d_R(\omega))^\top$. Marginalizing with respect to the random vector $(v_3(\omega), v_4(\omega), v_5(\omega))^\top = (b_R(\omega), b_C(\omega), d_R(\omega))^\top$ and taking $t > 0$ arbitrary, the 1-PDF of the solution SP $x(t,\omega)$ is

$$\begin{aligned}
&{}^{-}(x_R, x_C, t)\\
&= \int_{\mathbb{R}^-} \int_{\mathbb{R}^2} f_0\left(s_1(x_R, x_C, b_R, b_C, d_R), s_2(x_R, x_C, b_R, b_C, d_R), b_R, b_C, d_R\right)\\
&\quad \times \left|\sec(\sqrt{-d_R}t)\right| \mathrm{d}b_R\, \mathrm{d}b_C\, \mathrm{d}d_R.
\end{aligned} \tag{14}$$

Now, if $\mathbb{P}\left[\omega \in \Omega \,:\, d_R(\omega) > 0\right] = 1$, i.e. the random variable $d_R(\omega)$ has a strictly positive domain, the 1-PDF of the solution $x(t,\omega)$ is

$$\begin{aligned}
&f_1^+(x_R, x_C, t)\\
&= \int_{\mathbb{R}^+} \int_{\mathbb{R}^2} f_0\left(s_1(x_R, x_C, b_R, b_C, d_R), s_2(x_R, x_C, b_R, b_C, d_R), b_R, b_C, d_R\right)\\
&\quad \times \sec(\sqrt{d_R}t)^2 \mathrm{d}b_R\, \mathrm{d}b_C\, \mathrm{d}d_R,
\end{aligned} \tag{15}$$

being

$$s_1(x_R, x_C, b_R, b_C, d_R) = -\frac{b_R}{\sqrt{d_R}} + x_R \operatorname{sech}(t\sqrt{d_R}),$$

$$s_2(x_R, x_C, b_R, b_C, d_R) = x_C \operatorname{sech}(t\sqrt{d_R}) - \frac{b_C \tanh(t\sqrt{d_R})}{\sqrt{d_R}}.$$

As in the previous subsection, if $\mathbb{P}\left[\omega \in \Omega \,:\, d_R(\omega) > 0\right] \neq 1$ and $\mathbb{P}\left[\omega \in \Omega \,:\, d_R(\omega) < 0\right] \neq 1$, the 1-PDF of the solution SP is the sum of both functions Eqs. (14) and (15)

$$f_1(x_R, x_C, t) = f_1^+(x_R, x_C, t) + f_1^-(x_R, x_C, t).$$

Finally, if the coefficient d is zero in the IVP (5), the solution of the deterministic problem is $x(t) = a + bt$. Then, the real and complex components of $x(t)$ are

$$x_R(t) = a_R + b_R t, \qquad x_C(t) = a_C + b_C t.$$

Let $t > 0$ be fixed, to obtain the PDF of the random vector

$$(x_R(t,\omega), x_C(\omega))^\top = (a_R(\omega) + b_R(\omega)t, a_C(\omega) + b_C(\omega)t)^\top$$

in terms of the PDF of the random vector $\mathbf{u}(\omega) = (a_R(\omega), a_C(\omega), b_R(\omega), b_C(\omega))^\top$, we define the following deterministic mapping

$$\mathbf{r} : \mathbb{R}^4 \to \mathbb{R}^4, \qquad \begin{aligned}
v_1 &= r_1(\mathbf{u}) = a_R + b_R t,\\
v_2 &= r_2(\mathbf{u}) = a_C + b_C t,\\
v_3 &= r_3(\mathbf{u}) = b_R,\\
v_4 &= r_4(\mathbf{u}) = b_C.
\end{aligned}$$

Therefore, the inverse mapping $\mathbf{s} : \mathbb{R}^4 \to \mathbb{R}^4$ and its Jacobian are

$$\begin{aligned}
a_R &= s_1(\mathbf{v}) = v_1 - v_3 t,\\
a_C &= s_2(\mathbf{v}) = v_2 - v_4 t,\\
b_R &= s_3(\mathbf{v}) = v_3,\\
b_C &= s_4(\mathbf{v}) = v_4,
\end{aligned} \qquad J = 1.$$

Then, taking $t > 0$ arbitrary the 1-PDF of the solution SP $x(t,\omega)$ is

$$f_1(x_R, x_C, t) = \int_{\mathbb{R}^2} f_0(x_R - b_R t, x_C - b_C t, b_R, b_C)\, \mathrm{d}b_R\, \mathrm{d}b_C, \tag{16}$$

where $f_0(a_R, a_C, b_R, b_C)$ denotes the PDF of the random vector $(a_R(\omega), a_C(\omega), b_R(\omega), b_C(\omega))^\top$.

Following the same reasoning the 1-PDFs of the real and the complex components of the solution SP $x(t,\omega)$, in each of the scenarios, can be determined. For sake of generality in this study, calculations and formulas of that probabilistic distributions are exhibited in an appendix section, see Appendices A and B.

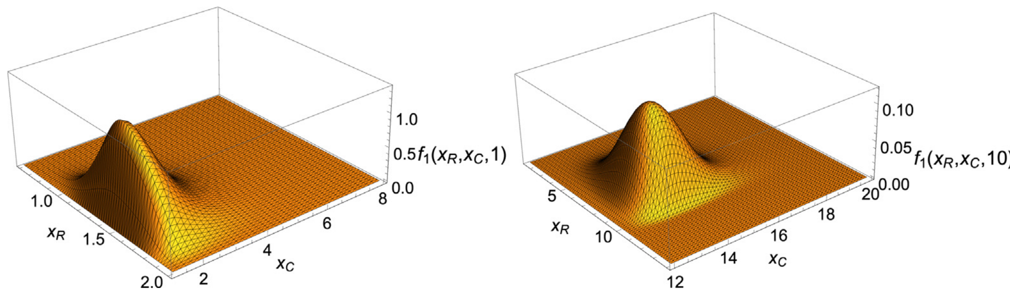

Fig. 1. PDF of the solution SP $x(t,\omega)$ at the time instants $t=1$ (left) and $t=10$ (right), in the context of Example 1. x_R and x_C are the values for the real and complex components, respectively.

4. Numerical examples

The aim of this section is to illustrate the capability of the theoretical results previously established in Section 3. We present four examples, with the aim of showing the random behaviour of the solution SP in the different scenarios indicated in Section 3. In the first and second examples independence between all RVs involved is assumed while in the third and fourth examples dependence is considered. We start assuming that $d = 0$ in IVP (5), that is we consider the third scenario being the roots $r_1 = r_2 = 0$. The computations are depicted in Example 1. In Example 2 we assume that the coefficient of the RDE (3) $d(\omega) = d_R(\omega)$ is a real RV, thus we are also considering the third scenario. In this case, the RV $d(\omega)$ affects to the dynamics of the solution SP by producing oscillatory trajectories. In the other two examples, we establish probabilistic distributions for the RV $d_C(\omega)$. In Example 3 we consider that $d_C(\omega)$ has a positive domain, then the roots indicated at the first scenario are considered. Example 4 is devoted to illustrate the case when the domain of RV $d_C(\omega)$ is the whole real line. In this case, as previously indicated in Section 3, the 1-PDF is computed by splitting the function into two parts, one part with the roots of the Scenario 1 and the other considering the roots of the Scenario 2. In all the numerical examples, the 1-PDFs of the solution SP $x(t,\omega)$, the real component $x_R(t,\omega)$ and the complex component $x_C(t,\omega)$ are computed. In addition, we also calculate the mean and the variance for each SP, see formulas in expression (1). For the SP $x(t,\omega)$ confidence regions are displayed, by applying formula (2), in order to show the evolution and variability of the randomized complex system under study.

Example 1. In this example we consider the particular case where the coefficient of the differential equation established in (5) is zero, i.e., $d = 0$. The initial conditions $a_R(\omega)$, $a_C(\omega)$, $b_R(\omega)$ and $b_C(\omega)$ are assumed to be independent RVs with the following distributions:

- $a_R(\omega)$ has an Uniform distribution on the interval $[0.5, 1]$, i.e., $a_R(\omega) \sim \mathrm{U}([0.5, 1])$.
- $a_C(\omega)$ has a Gamma distribution with parameters 2 and 0.5, i.e., $a_C(\omega) \sim \mathrm{Ga}(2, 0.5)$.
- $b_R(\omega)$ has a Beta distribution with parameters 7 and 3, i.e., $b_R(\omega) \sim \mathrm{Be}(7, 3)$.
- $b_C(\omega)$ has a Triangular distribution on the interval $[1.2, 1.5]$ with mode at 1.3, i.e., $b_C(\omega) \sim \mathrm{Tr}([1.2, 1.5], 1.3)$.

In Fig. 1 the PDF of the solution SP $x(t,\omega)$ is plotted at the fixed times instants $t = 1$ and $t = 10$. To figure both PDF, formula (16) is applied. In addition, from formulas (1) and (2) and the expression for the 1-PDF stated in Eq. (16), in Fig. 2 the expectation (blue points) and the 50% (red curve) and 90% (black curve) confidence regions are plotted for different time instants $t \in \{0, 1, 2, 5, 10\}$. We observe that the mean and the variability, in both components, increase over the time. Note that, the variability of the real component increase faster than the variability of the complex one. This agrees with the behaviour of 1-PDFs, of the real and complex components, plotted in Fig. 3. On the left part of this graphical representation the 1-PDF of $x_R(t,\omega)$ given in Eq. (A.2) is shown. On the right the 1-PDF of $x_C(t,\omega)$ given in Eq. (B.2) is represented. For the sake of clarity, in Fig. 4 the mean and the variance at the same time interval, $[0, 10]$, for the real (up) and the complex (bottom) components are plotted.

Example 2. In this example we consider the particular case where $d(\omega) = d_R(\omega)$ is a real RV. We assume that $a_R(\omega)$, $a_C(\omega)$, $b_R(\omega)$, $b_C(\omega)$ and $d_R(\omega)$ are independent RVs with the following distributions:

- $a_R(\omega)$ has an Uniform distribution on the interval $[0.5, 1]$, i.e., $a_R(\omega) \sim \mathrm{U}([0.5, 1])$.
- $a_C(\omega)$ has a Gamma distribution with parameters 2 and 0.5, i.e., $a_C(\omega) \sim \mathrm{Ga}(2, 0.5)$.
- $b_R(\omega)$ has a Beta distribution with parameters 7 and 3, i.e., $b_R(\omega) \sim \mathrm{Be}(7, 3)$.
- $b_C(\omega)$ has a Triangular distribution on the interval $[1.2, 1.5]$ with mode at 1.3, i.e., $b_C(\omega) \sim \mathrm{Tr}([1.2, 1.5], 1.3)$.
- $d_R(\omega)$ follows a truncated Gaussian distribution on the interval $[-10, 0]$ with mean -7 and standard deviation 0.05, i.e., $d_R(\omega) \sim \mathrm{N}_T(-7, 0.05)$ with $T = [-10, 0]$.

In this case, we choose $d_R(\omega)$ with a negative domain. Therefore, Eq. (14) is applied in order to compute the 1-PDF. In Fig. 5 the PDF of the solution SP $x(t,\omega)$ is plotted at the fixed times instants $t = 0.5$ and $t = 1.25$. From formulas (1) and (2) and the expression for the 1-PDF stated in Eq. (14), in Fig. 6 the expectation (blue points) and the 50% (red curve) and 90% (black curve) confidence regions are plotted for different instant times $t \in \{0, 0.5, 0.7, 0.9, 1.25\}$ (left) and $t \in \{1.5, 1.75, 1.9, 2.1, 2.5\}$ (right). We consider two sets of times to observe the oscillatory character of the complex system. We observe that, for the first time interval, in both components (real and complex) the mean decrease while the variability at first decreases and then rises again. In the second time interval considered, the mean increase in the both components, while the variability firstly decreases and then increases. We notice that there is a oscillatory behaviour in both, the mean and the variance. In addition, the variability of the complex component is bigger than that corresponding of the real one. This behaviour is in agreement with the 1-PDFs of the real and complex components plotted in Fig. 7. On the left part of this graphical representation the 1-PDF of $x_R(t,\omega)$ given in Eq. (A.2) is shown. On the right, the 1-PDF of $x_C(t,\omega)$ given in Eq. (B.2) is represented. For the sake of clarity, in Fig. 8 the mean and the variance at the same time interval, $[0, 1.25]$, for the real (up) and the complex (bottom) components are plotted. Notice that, although the mean and the variance of $x_R(t,\omega)$ and $x_C(t,\omega)$ have a similar shape, with a different scale, the 1-PDFs are different. Recall in this point the importance of computing the 1-PDF, which gives us a full probabilistic description of the SP. In all these graphical representations we show the behaviour of the complex system consider in a neighbourhood of the initial time instant $t = 0$. Finally, to see what happens with bigger times, in Fig. 9 the mean and the variance of the real and the complex components are depicted on the time interval $[0, 20]$. We observe that the expectations have a oscillatory behaviour, with a certain periodicity. The variance of both components also tends to increase in an oscillating manner.

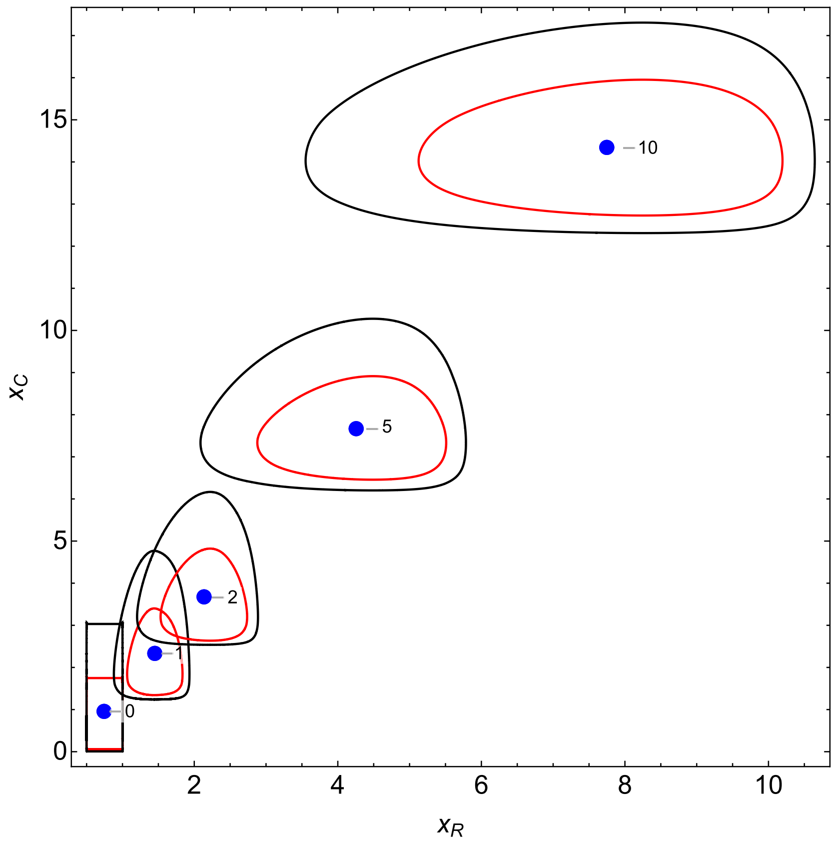

Fig. 2. Blue points represent the expectation of the solution SP for different time instants $t_i \in \{0, 1, 2, 5, 10\}$, $\mathbb{E}\left[x(t_i, \omega)\right]$. 50% (red curve) and 90% (black curve) confidence regions are plotted for each instant time t_i. x_R and x_C are the values for the real and complex components, respectively. This graphical representation has been done in the context of Example 1. (For interpretation of the references to colour in this figure legend, the reader is referred to the web version of this article.)

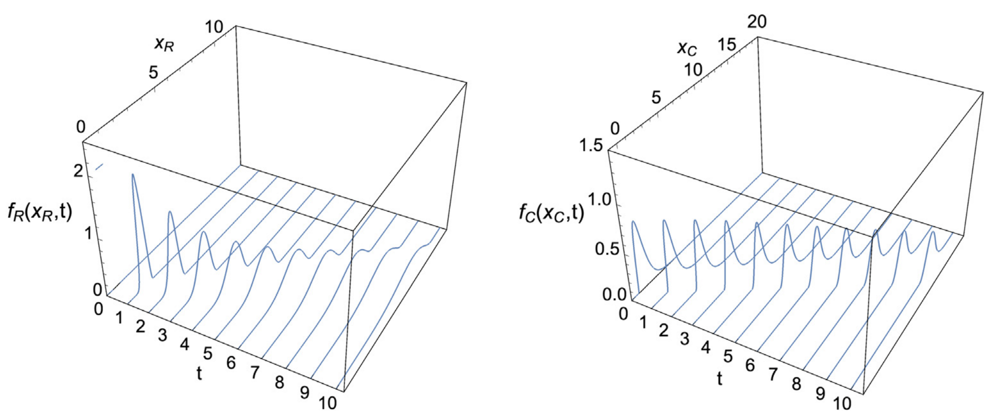

Fig. 3. PDFs of the real component $x_R(\omega)$ (left) and the complex component $x_C(\omega)$ (right) of the solution SP of the IVP (3)–(4) at the time instants $t_i \in \{0, 1, 2, \dots, 10\}$, in the context of Example 1.

Example 3. In the next example, we assume the following distributions for the random input parameters:

- The random vector $(a_R(\omega), a_C(\omega))$ follows a Multivariate Normal distribution with mean $\mu = (1, 1)^\top$ and variance–covariance matrix

$$\Sigma = \frac{1}{20}\begin{pmatrix} 1 & 0.1 \\ 0.1 & 1 \end{pmatrix}.$$

  That is, $(a_R(\omega), a_C(\omega)) \sim \mathrm{N}(\mu, \Sigma)$.
- The random vector $(b_R(\omega), b_C(\omega))$ has a Multivariate Uniform distribution in the rectangle $[1, 2] \times [2, 3]$, i.e, $(b_R(\omega), b_C(\omega)) \sim \mathrm{U}([1, 2], [2, 3])$.
- The random variable $d_R(\omega)$ has a Beta distribution with parameters 2 and 3, i.e., $d_R(\omega) \sim \mathrm{Be}(2, 3)$.
- $d_C(\omega)$ has a Gamma distribution with parameters 4 and 5, i.e., $d_C(\omega) \sim \mathrm{Ga}(4, 5)$.

In this case, $\mathbb{P}\left[\omega \in \Omega \,:\, d_C(\omega) > 0\right] = 1$. Therefore, the roots indicated in the Scenario 1 has been used in the formula of the 1-PDF of the solution SP given in Eq. (11), i.e., we consider Eq. (12). In Fig. 10 the PDF of the solution SP $x(t, \omega)$ is depicted at the fixed times instants $t = 0.05$ and $t = 0.35$. In addition, in Fig. 11 the expectation (blue point) and the 50% (red curve) and 90% (black curve) confidence regions are plotted for different instant times $t = \{0, 0.05, 0.1, 0.15, 0.2, 0.25, 0.3, 0.25\}$. The mean and the confidence region have been obtained from formulas (1), (2) and (12), where the 1-PDF of the solution SP, $f_1(x_R, x_C, t)$ has

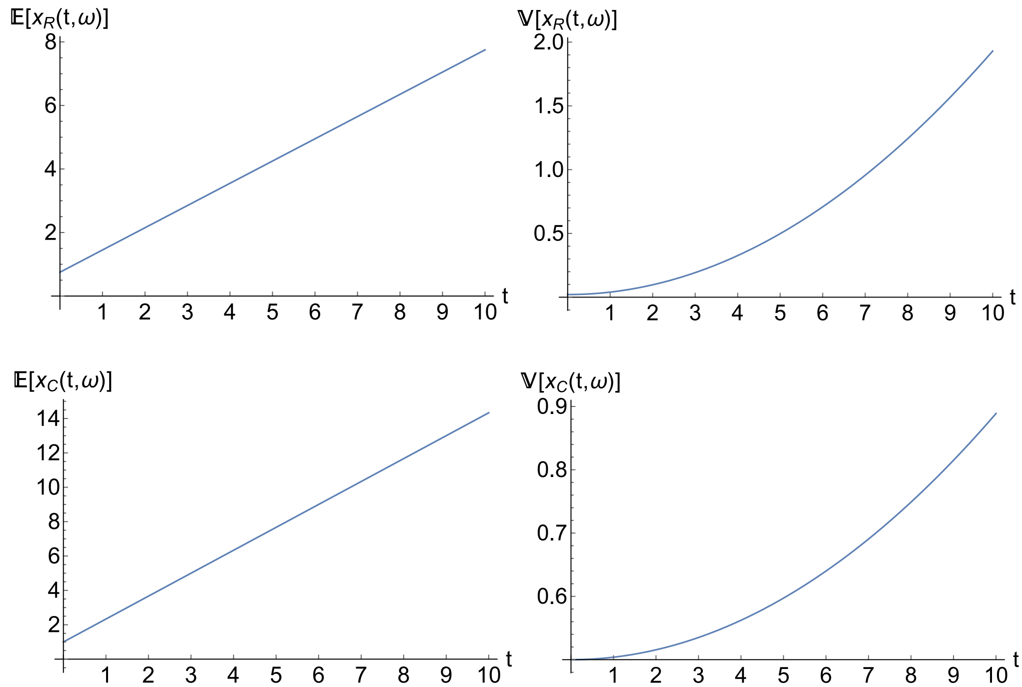

Fig. 4. Expectation (left) and variance (right) of the real and complex components of the solution SP $x(t,\omega)$ (top and bottom, respectively) at the time interval $[0,10]$, in the context of Example 1.

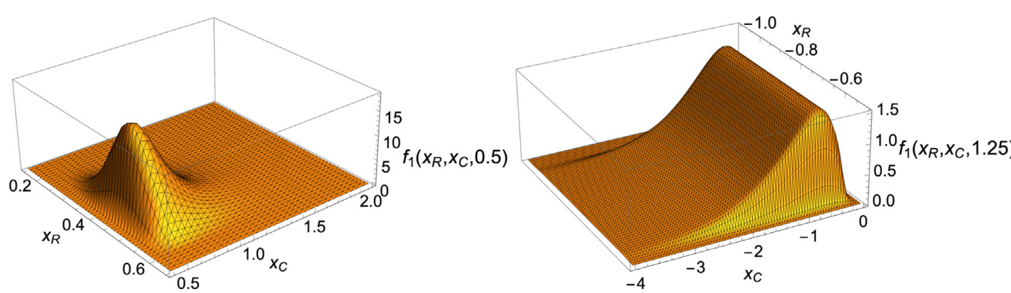

Fig. 5. PDF of the solution SP $x(t,\omega)$ at the time instants $t = 0.5$ (left) and $t = 1.25$ (right), in the context of Example 2. x_R and x_C are the values for the real and complex components, respectively.

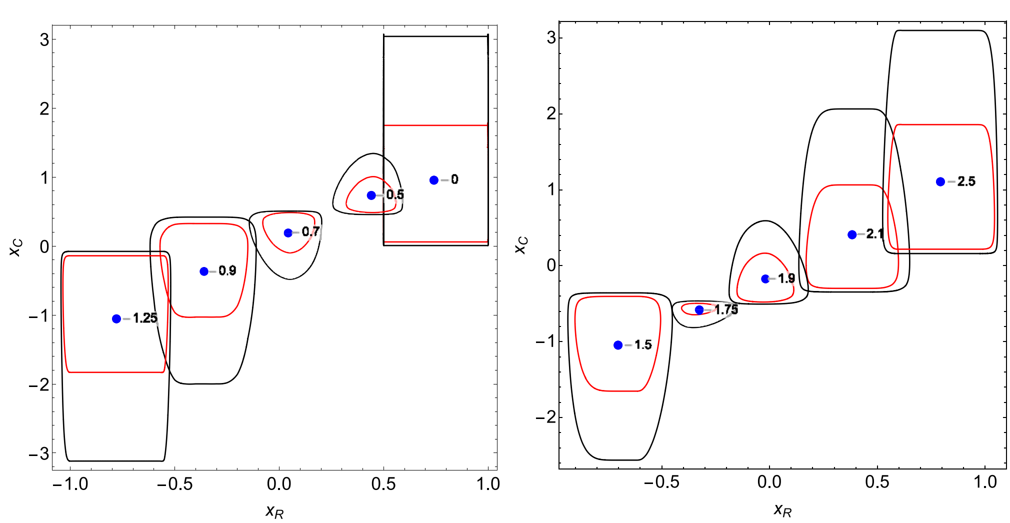

Fig. 6. Blue points represent the expectation of the solution SP, $\mathbb{E}\left[x(t_i,\omega)\right]$, for different time instants $t_i \in \{0, 0.5, 0.7, 0.9, 1.25\}$ (left) and $t_i \in \{1.5, 1.75, 1.9, 2.1, 2.5\}$ (right). 50% (red curve) and 90% (black curve) confidence regions are plotted for each instant time t_i. x_R and x_C are the values for the real and complex components, respectively. This graphical representation has been done in the context of Example 2. (For interpretation of the references to colour in this figure legend, the reader is referred to the web version of this article.)

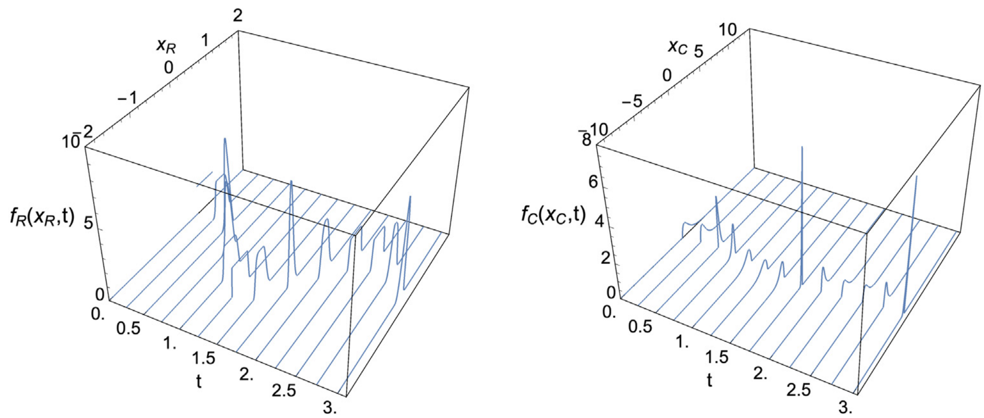

Fig. 7. PDFs of the real component $x_R(\omega)$ (left) and the complex component $x_C(\omega)$ (right) of the solution SP of the IVP (3)–(4) at the time instants $t_i \in \{0, 0.25, \dots, 3\}$, in the context of Example 2.

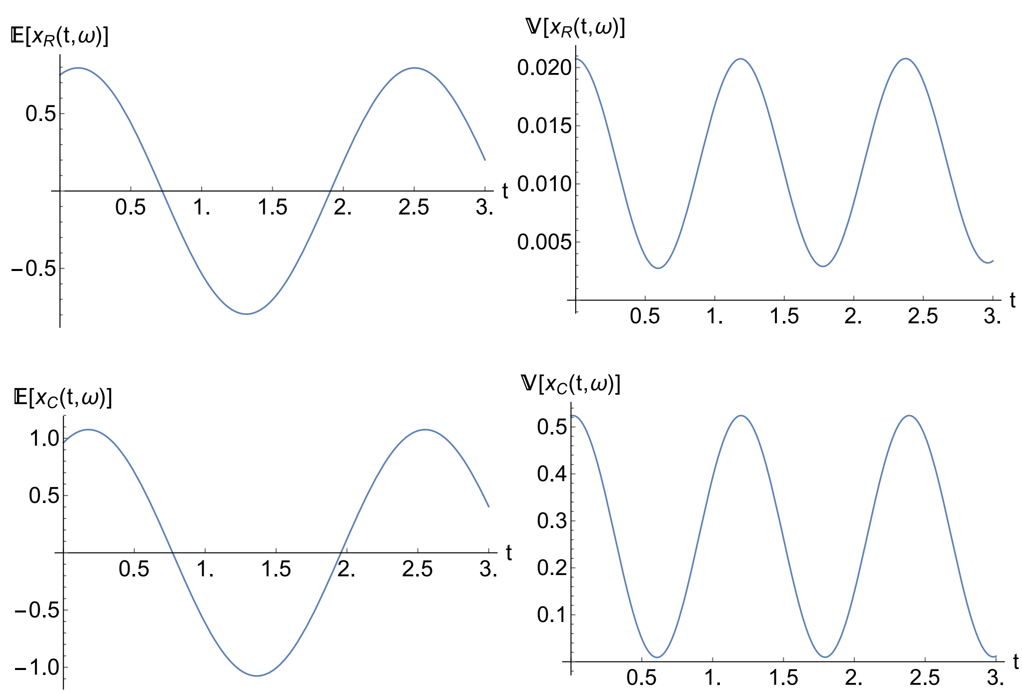

Fig. 8. Expectation (left) and variance (right) of the real and complex components of the solution SP $x(t,\omega)$ (top and bottom, respectively) at the time interval $[0,3]$, in the context of Example 2.

been established. We can observe that the variability increases over the time while the mean moves away from zero. In Fig. 12 the 1-PDFs of the real and complex components are plotted. On the left, the 1-PDF of $x_R(t,\omega)$ given in Eq. (A.1) is shown. On the right, the 1-PDF of $x_C(t,\omega)$ established in Eq. (B.1) is represented. In the interest of clarity, in Fig. 13 the mean and the variance for the real (up) and the complex (bottom) components are pictured in the interval $[0, 0.35]$. We see that, at the chosen time interval, the mean of the real component decrease while the mean of the complex component increase over time. In addition, in both components the variability augments. This behaviour is consistent with that shown in Fig. 11. For times further from zero, see Fig. 14 we observe that the mean and the variance grow exponentially for both the real and complex components. In addition, the expectation diverge oscillating in both contributions, the real and the complex.

Example 4. To finish, we show an example where the domain of $d_C(\omega)$ is the whole real line. We consider the following IVP

$$\begin{cases} \ddot{x}(t,\omega) - d(\omega)x(t,\omega) = 0, & t > 0, \\ x(0) = a_C(\omega)\,\mathrm{i}, & \dot{x}(0) = b_R(\omega). \end{cases}$$

where $d(\omega)$ is a absolutely continuous complex RV, $d(\omega) = d_R(\omega) + \mathrm{i}\, d_R(\omega)$, and $a_C(\omega)$ and $b_R(\omega)$ are absolutely continuous real RVs, all defined in a complete probability space $(\Omega, \mathcal{F}, \mathbb{P})$. We assume that the random vector $(d_R(\omega), d_C(\omega))$ has a Multivariate Gaussian distribution with mean $\mu = (0, 0.5)^\top$ and variance–covariance matrix

$$\Sigma = \frac{1}{20}\begin{pmatrix} 1 & 0.2 \\ 0.2 & 2 \end{pmatrix}.$$

That is, $(d_R(\omega), d_C(\omega)) \sim \mathrm{N}(\mu, \Sigma)$. For the real RVs $a_C(\omega)$ and $b_R(\omega)$ we consider the following distributions

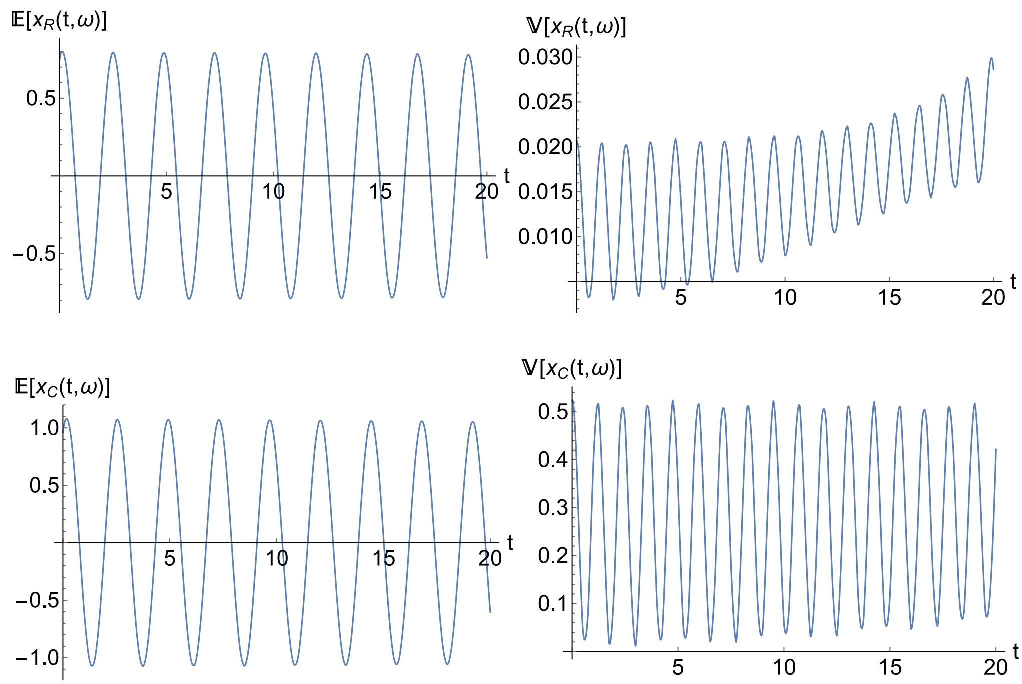

Fig. 9. Expectation (left) and variance (right) of the real and complex components of the solution SP $x(t,\omega)$ (top and bottom, respectively) at the time interval $[0,20]$, in the context of Example 2.

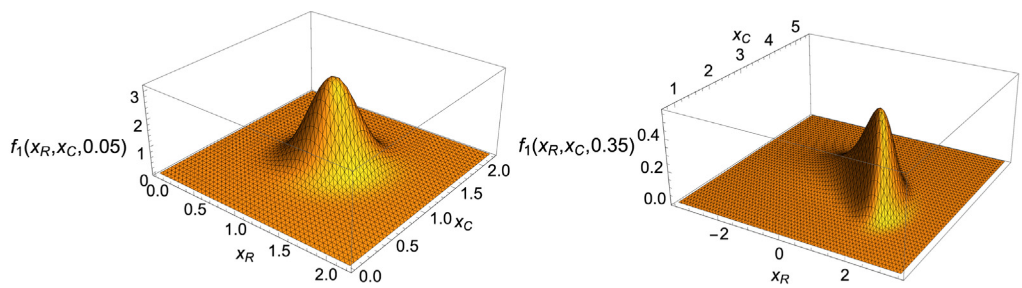

Fig. 10. PDF of the solution SP $x(t,\omega)$ at the time instants $t=0.05$ (left) and $t=0.35$ (right), in the context of Example 3. x_R and x_C are the values for the real and complex components, respectively.

- $a_C(\omega) \sim \mathrm{Be}(2,2)$.
- $b_R(\omega) \sim \mathrm{Ga}(4,4)$.

As the RV $d_C(\omega)$ gets both positive and negative values, the 1-PDF of the solution SP $x(t,\omega)$ is split into two parts, i.e.,

$$f_1(x_R,x_C,t) = f_1^+(x_R,x_C,t) + f_1^-(x_R,x_C,t),$$

where $f_1^+(x_R,x_C,t)$ and $f_1^-(x_R,x_C,t)$ are established in Eq. (12) and (13), respectively. Therefore, to compute $f_1^+(x_R,x_C,t)$ we consider the positive values of the domain of the RV $d_C(\omega)$ and to obtain $f_1^-(x_R,x_C,t)$ the negative. In this point, highlight that both functions $f_1^+(x_R,x_C,t)$ and $f_1^-(x_R,x_C,t)$ are not probabilistic distributions. They are the positive and negative contributions of the 1-PDF $f_1(x_R,x_C,t)$ and the following is fulfilled for every $t>0$ fixed

$$\int_{\mathbb{R}^2} f_1(x_R,x_C,t)\,\mathrm{d}x_R\,\mathrm{d}x_C = \int_{\mathbb{R}^2} f_1^+(x_R,x_C,t)\,\mathrm{d}x_R\,\mathrm{d}x_C + \int_{\mathbb{R}^2} f_1^-(x_R,x_C,t)\,\mathrm{d}x_R\,\mathrm{d}x_C = 1.$$

In this example, from the calculation of the corresponding probabilities, it is evident that the positive contribution is more significant than the negative

$$\mathbb{P}\left[\omega\in\Omega\ :\ d_C(\omega)>0\right] = 0.943077, \quad \mathbb{P}\left[\omega\in\Omega\ :\ d_C(\omega)<0\right] = 0.056923.$$

The PDF of the solution SP $x(t,\omega)$ is plotted in Fig. 15 at the fixed times $t=0.2$ and $t=0.6$. In addition, in Fig. 16 the expectation (blue point) and the 50% (red curve) and 90% (black curve) confidence regions are plotted for different instant times $t\in\{0,0.05,0.1,0.15,0.2,0.25,0.3,0.25\}$. The mean and the confidence region have been obtained from formulas (1) and (2), Eqs. (12) and (13). We see that both the expectation and variability grow as time passes, in both components the real and the complex. This behaviour agrees with the shown in Fig. 17 and Fig. 18. In Fig. 17 the 1-PDFs of the real and the complex components are represented for different time instant $t\in\{0.2,0.4,0.6,0.8,1\}$. The expectation and variance at the time interval $[0.2,1]$ are depicted in Fig. 18. Finally, in Fig. 19 we observe that for large times the expectation of the real and complex components diverge oscillating. For both components the variance growths exponentially.

5. Application to the simple harmonic oscillator

As indicated at the introduction, complex differential equations have a significant role in Engineering. In this section, we apply the results obtained in Section 3 to the simple harmonic oscillator defined on the complex domain. This model is certainly the simplest model to examine dynamical systems in engineering but it is fundamental to understand most of the physical phenomena [25]. For example, let

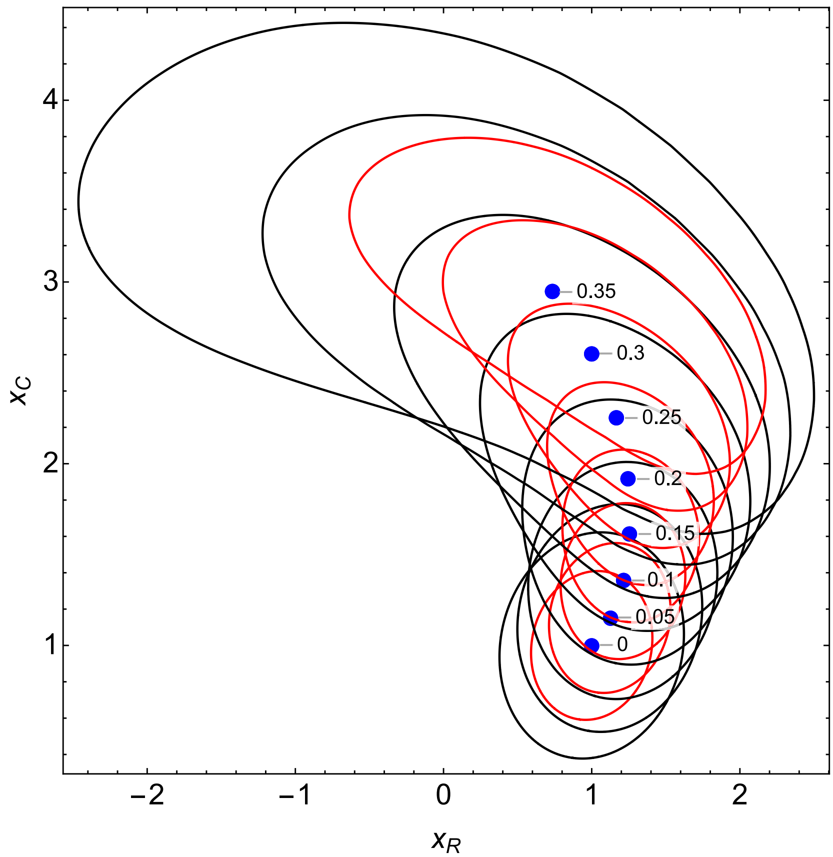

Fig. 11. Blue points represent the expectation of the solution SP for different time instants $t_i \in \{0, 0.05, 0.1, 0.15, 0.2, 0.25, 0.3, 0.35\}$, $\mathbb{E}\left[x(t_i, \omega)\right]$. 50% (red curve) and 90% (black curve) confidence regions are plotted for each instant time t_i. x_R and x_C are the values for the real and complex components, respectively. This graphical representation has been done in the context of Example 3. (For interpretation of the references to colour in this figure legend, the reader is referred to the web version of this article.)

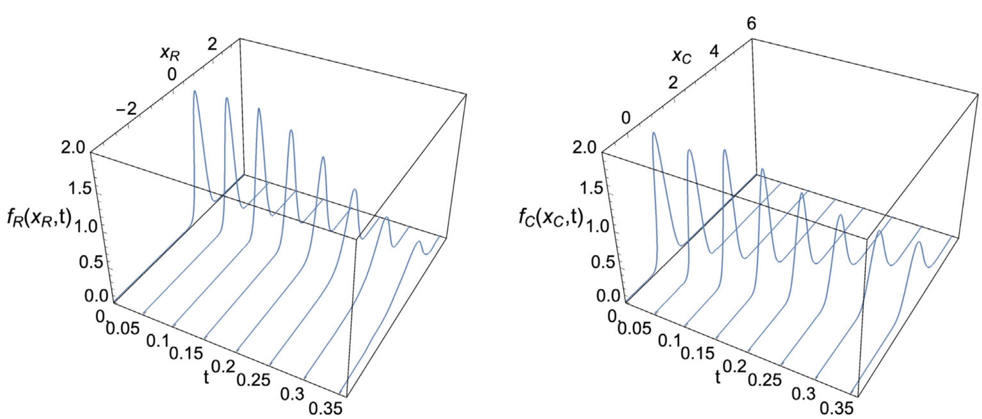

Fig. 12. PDFs of the real component $x_R(\omega)$ (left) and the complex component $x_C(\omega)$ (right) of the solution SP of the IVP (3)–(4) at the time instants $t_i \in \{0, 0.05, 0.1, 0.15, 0.2, 0.25, 0.3, 0.35\}$, in the context of Example 3.

m be a mass joined to one end of a massless spring (or pendulum) with stiffness constant k. The other end of the spring is assumed to be immobilized. Then, the equation of motion of this simple harmonic oscillator is

$$\ddot{x}(t) + \omega_0^2 x(t) = 0, \quad t > 0, \tag{17}$$

where $\omega_0^2 = k/m$. Differential Eq. (17) has multiple applications in the complex domain. For instance, in the analysis of electrical circuits. Consider an LC circuit which consists of and inductor and a capacitor and, denote by L and C the inductance and the capacitance of the inductor and capacitor components, respectively. In this case, the differential equation writes as

$$\ddot{I}(t) + \frac{1}{LC} I(t) = 0, \quad t > 0, \tag{18}$$

being $I(t)$ the current in the circuit at the time instant t. Depending on the nature of the problem which we are dealing with, it can be assumed that L and/or C are complex numbers, see [26,27]. Then, in this case $\omega_0 = 1/\sqrt{LC}$ is called the resonant frequency of the LC circuit, and it is also complex.

In relation of the densities of the random parameters, we consider $\omega_0^2(\omega) = -d(\omega) = -\mathrm{i}\, d_C(\omega)$, where $d_C(\omega)$ has a Gaussian distribution with mean -900 and a 20% of variability, i.e, $d_C(\omega) \sim \mathrm{N}(-900, 900p)$, $p = 0.2$. Regarding the initial conditions $x(0, \omega) = a_R(\omega) + \mathrm{i}\, a_C(\omega)$ and

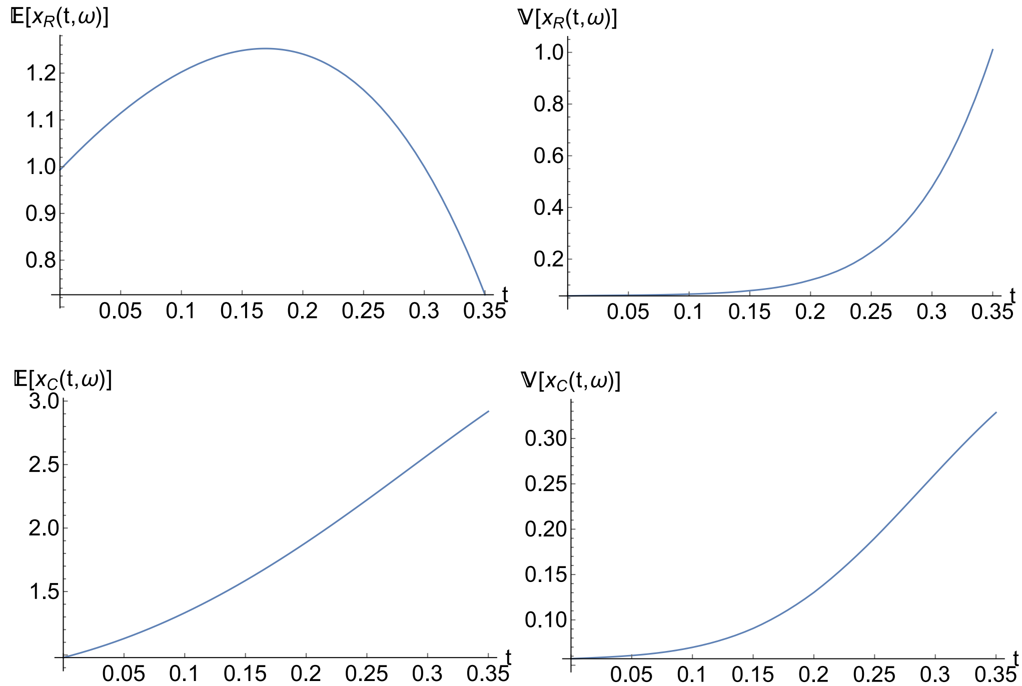

Fig. 13. Expectation (left) and variance (right) of the real and complex components of the solution SP $x(t,\omega)$ (top and bottom, respectively) at the time interval $[0, 0.25]$, in the context of Example 3.

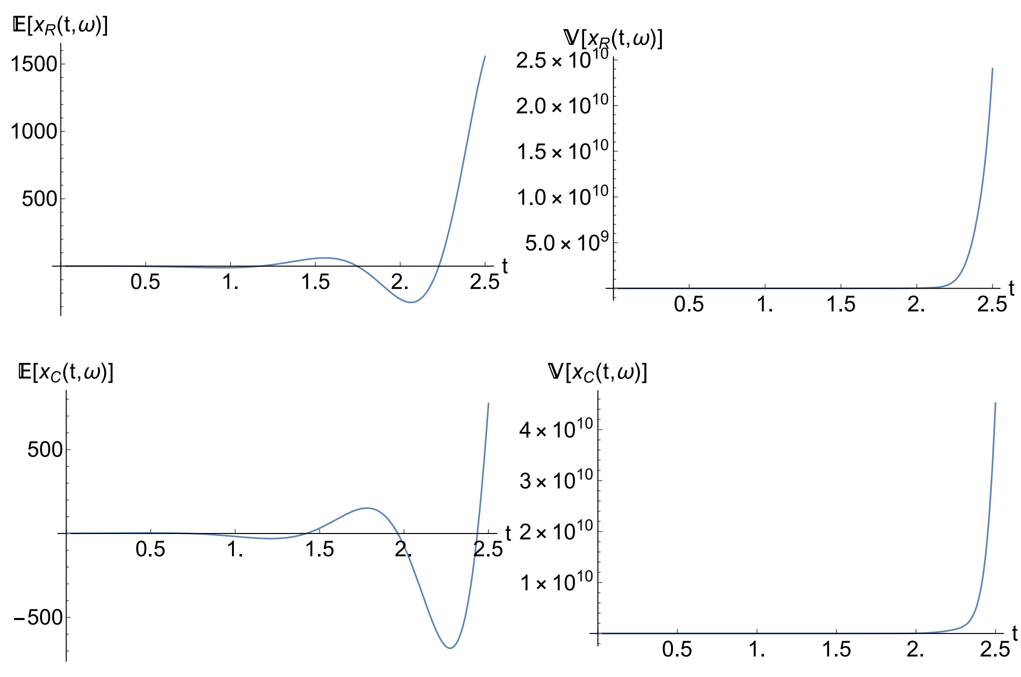

Fig. 14. Expectation (left) and variance (right) of the real and complex components of the solution SP $x(t,\omega)$ (top and bottom, respectively) at the time interval $[0, 2.5]$, in the context of Example 3.

$\dot{x}(0,\omega) = b_R(\omega) + \mathrm{i}\, b_C(\omega)$, for sake of simplicity we assume that a_C, b_R and b_C are deterministic and equal to zero. Then, only randomness is assumed in $x(0,\omega) = a_R(\omega)$, where $a_R(\omega)$ follows a Gamma distribution with parameters 5 and 0.2 i.e., $a_R(\omega) \sim \mathrm{Ga}(5, 0.2)$. Note that, to determine the expression of the 1-PDF of the solution SP, the PDF of both $a_R(\omega)$ and $a_C(\omega)$ are necessary, since we shall define a one-to-one transformation. As $a_C = 0$, then it density can be defined from the Dirac delta function as follows

$$f_{a_C}(a_C) = \delta(a_C), \quad -\infty < a_C < \infty.$$

In this application we compute the PDF of the solution SP $x(t,\omega)$, and the densities of the real and complex components of the solution, for different time instants. The results are compared with those obtained using Monte Carlo simulation (MCS), which is a common alternative to calculate densities, [28–30]. Although widely used due to easy implementation, the main drawback of MCS methods is that the accuracy depends on the sampling say. That is, it has a slow convergence rate $\mathcal{O}(1/\sqrt{M})$, M being the number of simulations. Thus, bigger samples give us more accurate results but increasing the related computational effort. In addition, MCS only provides numerical approximations of

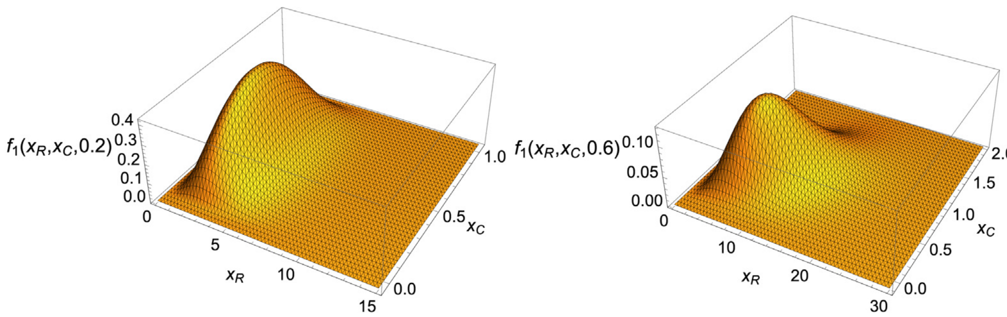

Fig. 15. PDF of the solution SP $x(t,\omega)$ at the time instants $t = 0.2$ (left) and $t = 0.6$ (right), in the context of Example 4. x_R and x_C are the values for the real and complex components, respectively.

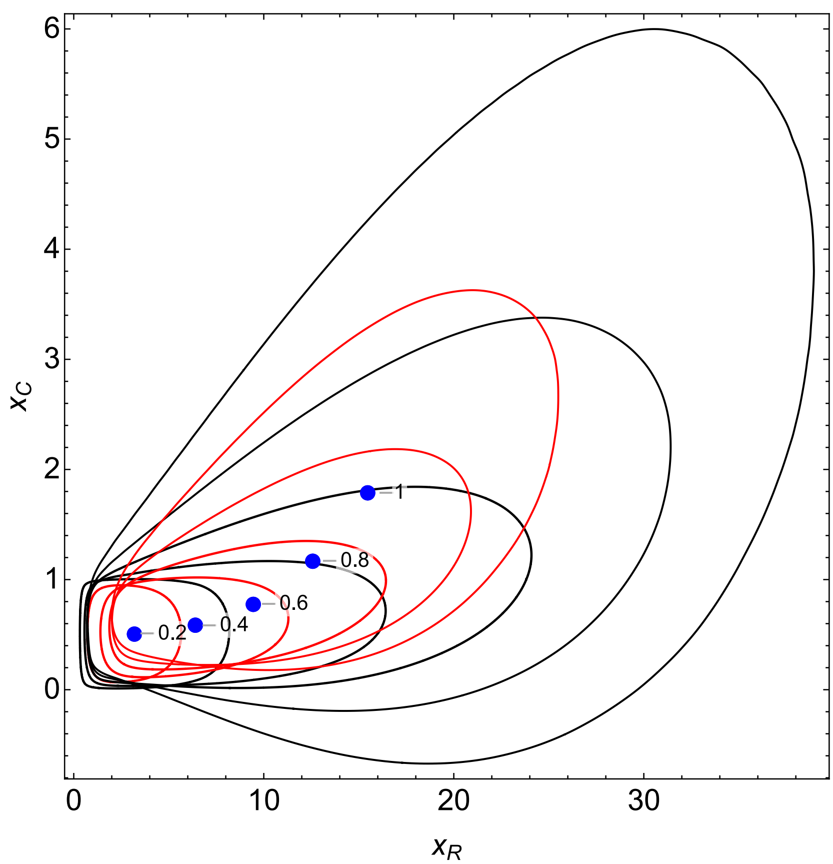

Fig. 16. Blue points represent the expectation of the solution SP for different time instants $t_i \in \{0.2, 0.4, 0.6, 0.8, 1\}$, $\mathbb{E}\left[x(t_i,\omega)\right]$. 50% (red curve) and 90% (black curve) confidence regions are plotted for each instant time t_i. x_R and x_C are the values for the real and complex components, respectively. This graphical representation has been done in the context of Example 4. (For interpretation of the references to colour in this figure legend, the reader is referred to the web version of this article.)

solution SP in spite of an exact representation could exist, as obtained in this contribution.

In Fig. 20 the PDF of the solution SP $x(t,\omega)$ is plotted at the times instants $t = 0.01$ and $t = 0.4$. The PDF have been obtained using the RVT method, from the theoretical results stated in Section 3, and the classical MCS, considering 10^6 samples. We can observe that the analytical computations obtained by applying the RVT method agree with MCS, the first method being more accurate. We see that for the time instant $t = 0.4$ the PDF takes smaller values than at the time instant $t = 0.01$, what means that there is more variability. This conclusion is in agreement with Fig. 21, where the PDF of the real and complex components of the solution SP are represented at both times instants $t = 0.01$ and $t = 0.4$. In both graphical representations, Fig. 20 and Fig. 21, we show that applying the RVT method the exact density is calculated, while with MCS an approximation is obtained. Finally, in Fig. 22 the behaviour of the expectation and the variance of the solution SP $x(t,\omega) = x_R(\omega) + \mathrm{i}\, x_C(\omega)$ are plotted in the time interval $[0, 0.5]$. In order to see the behaviour at the first times, we also have plotted it in the time interval $[0, 0.15]$. We observe that both quantities the expectation and the variance increase over the time, with the growth of the expectation being oscillatory.

6. Conclusions and future work

In this paper we take advantage of the Random Variable Transformation technique to determine an exact expression of the first probability density function of the solution stochastic process of a randomized linear second-order differential equation with complex coefficients. The first probability density function provided us a full probabilistic description of the solution stochastic process. From it we can obtain important statistical information such as the mean, variability and confidence regions. For the sake of generality, the theoretical

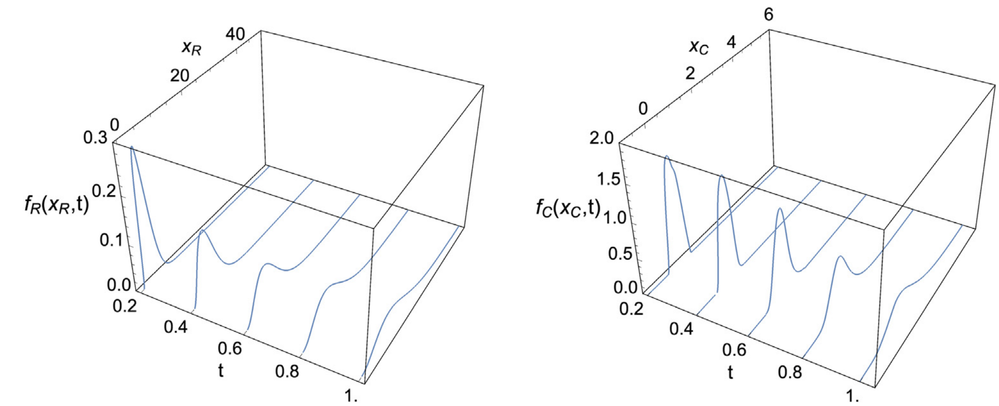

Fig. 17. PDFs of the real component $x_R(\omega)$ (left) and the complex component $x_C(\omega)$ (right) of the solution SP of the IVP (3)–(4) at the time instants $t_i \in \{0.2, 0.4, 0.6, 0.8, 1\}$, in the context of Example 4.

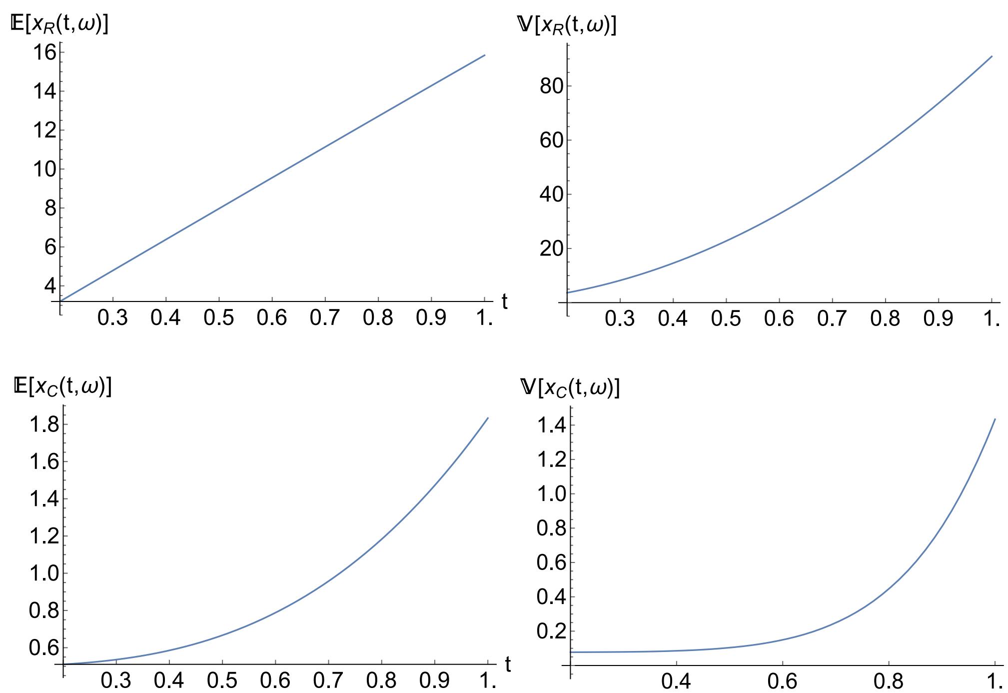

Fig. 18. Expectation (left) and variance (right) of the real and complex components of the solution SP $x(t,\omega)$ (top and bottom, respectively) at the time interval $[0.2, 1]$, in the context of Example 4.

analysis has been done considering all the possible scenarios motivated by the deterministic theory. The results in this paper have a great potential regarding applications. For instance, second-order differential equations are key tools in Engineering. And, considering uncertainty in its formulation is necessary to take into account inherent errors. In this contribution, the capability of theoretical results established has been demonstrated via numerous numerical examples and a particular application where the simple harmonic oscillator, defined on the complex domain, is considered. In the application, the first probability density function of the response is calculated using two methods: the results obtained applying the random variable transformation technique and Monte Carlo simulations. We show how with the first method give us more accurate results. In a future contribution, the next natural step is to consider the non-homogeneous system. In addition, we plan to go a step forward by analysing other interesting linear or no-linear differential equations with random complex coefficients, such as the Riccati differential equation.

Declaration of competing interest

The authors declare that they have no known competing financial interests or personal relationships that could have appeared to influence the work reported in this paper.

Acknowledgements

This work has been supported by the grant PID2020-115270GB–I00 funded by MCIN/AEI/10.13039/501100011033, Spain and the grant AICO/2021/302 (Generalitat Valenciana).

Appendix A. Computing the 1-PDF of the real component, $x_R(t,\omega)$

In this appendix the 1-PDF of the real component $x_R(t,\omega)$ is determined. First, we compute the 1-PDF in the first and second scenarios indicated in the introduction, that is, we consider $d_C(\omega)$ a continuous RV. After that, we will assume that the RV $d(\omega) = d_R(\omega)$ has only a real

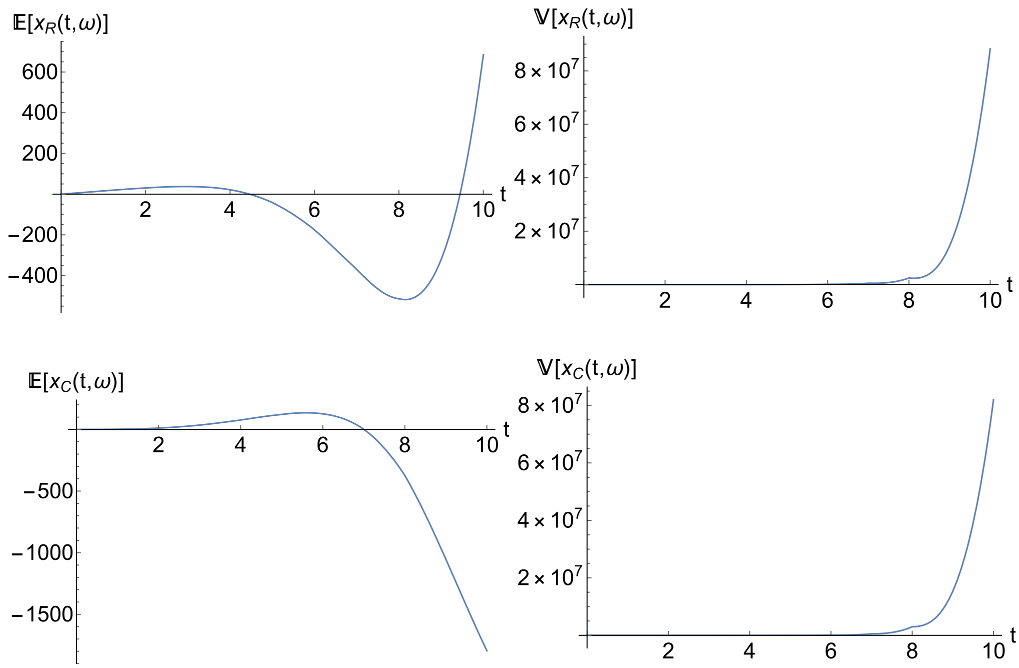

Fig. 19. Expectation (left) and variance (right) of the real and complex components of the solution SP $x(t,\omega)$ (top and bottom, respectively) at the time interval $[0,10]$, in the context of Example 4.

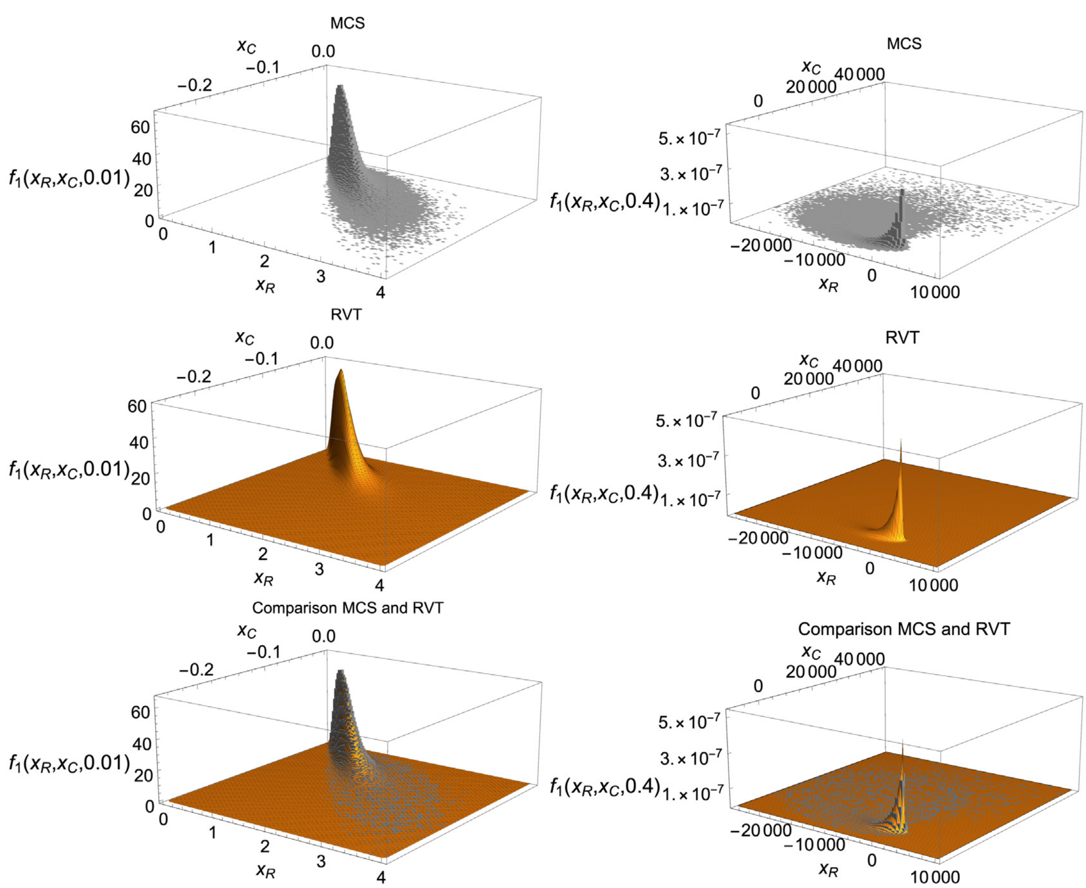

Fig. 20. PDF of the solution SP $x(t,\omega)$ at the time instants $t = 0.01$ (left) and $t = 0.4$ (right), in the context of the application stated in Section 5. Top: Applying the RVT method; Middle: Applying MCS; Bottom: Comparison between MCS and RVT. x_R and x_C are the values for the real and complex components, respectively.

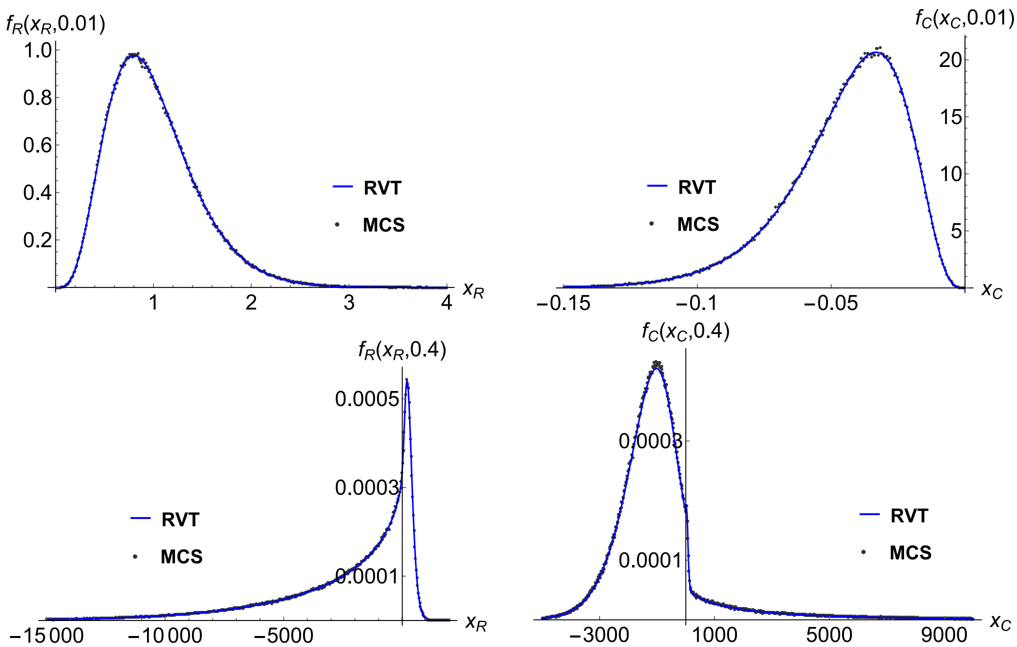

Fig. 21. PDFs of the real component $x_R(\omega)$ (left) and the complex component $x_C(\omega)$ (right) of the solution SP of the IVP (3)–(4) at the time instants $t = 0.01$ (top) and $t = 0.4$ (bottom), in the context of the application stated in Section 5. Comparison between RVT (blue line) and MCS (black points). (For interpretation of the references to colour in this figure legend, the reader is referred to the web version of this article.)

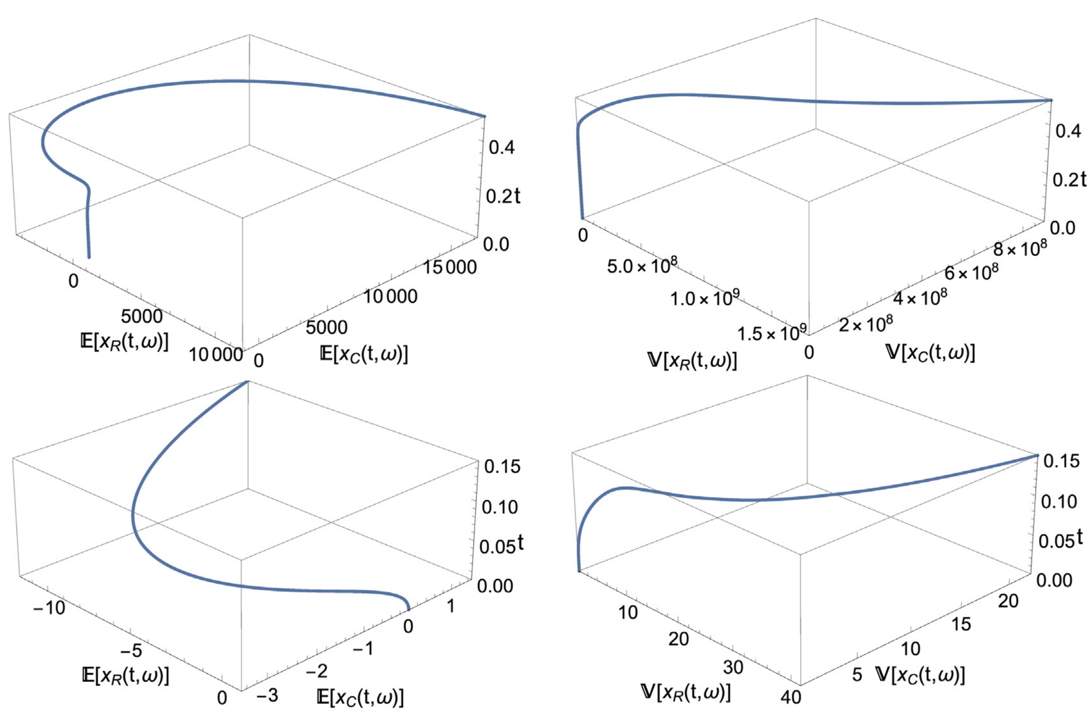

Fig. 22. Expectation (left) and variance (right) of the real and complex components of the solution SP $x(t,\omega)$ at the time intervals $[0,0.5]$ and $[0,0.15]$ (top and bottom, respectively), in the context of the application stated in Section 5.

contribution. Finally, we consider that the RV $d(\omega)=0$ for all $\omega\in\Omega$. That is, the coefficient d is zero in the IVP (5).

A.1. Computing the 1-PDF in the first and second scenarios

In this case, the real component $x_R(t,\omega)$ is given in Eq. (8). Let $t>0$ be fixed, we apply the RVT method, Theorem 1, to the mapping $\mathbf{r}:\mathbb{R}^6\to\mathbb{R}^6$

$$\begin{aligned} v_1 &= r_1(\mathbf{u}) = x_R(t) = a_R g_1(t;\mathbf{y}) + a_C g_2(t;\mathbf{y}) + g_3(t;\mathbf{y}),\\ v_2 &= r_2(\mathbf{u}) = a_C,\\ \hat{\mathbf{v}} &= \hat{\mathbf{r}}(\mathbf{u}) = \mathbf{y}, \end{aligned}$$

where $\hat{\mathbf{v}}=(v_3,v_4,v_5,v_6)$, $\hat{\mathbf{r}}=(r_3,r_4,r_5,r_6)$ and $\mathbf{y}=(b_R,b_C,d_R,d_C)$. The inverse mapping $\mathbf{s}:\mathbb{R}^6\to\mathbb{R}^6$, $\mathbf{s}=(s_1,s_2,\hat{\mathbf{s}})$, is

$$\begin{aligned} a_R &= s_1(\mathbf{v}) = \frac{v_1 - v_2 g_2(t;\hat{\mathbf{v}}) - g_3(t;\hat{\mathbf{v}})}{g_1(t;\hat{\mathbf{v}})},\\ a_C &= s_2(\mathbf{v}) = v_2,\\ \mathbf{y} &= \hat{\mathbf{s}}(\mathbf{v}) = \hat{\mathbf{v}}. \end{aligned}$$

The Jacobian of the mapping $\mathbf{s}$ is

$$J=\frac{1}{g_1(t,\hat{\mathbf{v}})}=\frac{1}{\cos(r_{1C}t)\cosh(r_{1R}t)}=\frac{\sec(r_{1C}t)}{\cosh(r_{1R}t)},$$

where $r_{1R}=r_{1R}(v_5,v_6)$ and $r_{1C}=r_{1C}(v_5,v_6)$ are the real and complex part of the root $r=\sqrt{d_R+id_C}=\sqrt{v_5+iv_6}$. Then, the PDF of the random vector $\mathbf{v}$ in terms of the PDF of input parameters is

$$f_{\mathbf{v}}(\mathbf{v})=f_0\left(s_1(\mathbf{v}),v_2,\hat{\mathbf{v}}\right)\left|\frac{\sec(r_{1C}t)}{\cosh(r_{1R}t)}\right|.$$

Marginalizing with respect to the random vector $(v_2(\omega),\hat{\mathbf{v}}(\omega))^\top$ and taking $t>0$ arbitrary, the 1-PDF of the real component of the solution SP of IVP (3)–(4) is

$$f_R(x_R,t)=\int_{\mathbb{R}^5} f_0\left(s_1(x_R,a_C,\mathbf{y}),a_C,\mathbf{y}\right)\left|\frac{\sec(r_{1C}(d_R,d_C)t)}{\cosh(r_{1R}(d_R,d_C)t)}\right|\mathrm{d}a_C\,\mathrm{d}\mathbf{y}, \quad \text{(A.1)}$$

where $\mathbf{y}=(b_R,b_C,d_R,d_C)$. As it has been indicated in Section 3, depending on the domain of the RV $d_C(\omega)$, we consider the roots of the first scenario, the second scenario or both (splitting the 1-PDF into two parts, the positive and negative).

A.2. Computing the 1-PDF in the third scenario

We compute the 1-PDF in the third scenario, considering that the coefficient of the RDE (3) is a real RV, $d(\omega)=d_R(\omega)$. If $d_R(\omega)$ is a RV with negative domain, the 1-PDF is

$$\begin{aligned} f_R^-(x_R,t)=&\int_{\mathbb{R}^-}\int_{\mathbb{R}} f_{0R}\left(\frac{\sec(\sqrt{-d_R}t)\left(\sqrt{-d_R}x_R-b_R\sin(\sqrt{-d_R}t)\right)}{\sqrt{-d_R}},b_R,d_R\right)\\ &\times\left|\sec(\sqrt{-d_R}t)\right|\mathrm{d}b_R\,\mathrm{d}d_R. \end{aligned} \quad \text{(A.2)}$$

On the other hand, if $\mathbb{P}\left[\omega\in\Omega\,:\,d_R(\omega)>0\right]=1$, the 1-PDF is given by

$$\begin{aligned} f_R^+(x_R,t)=&\int_{\mathbb{R}^+}\int_{\mathbb{R}} f_{0R}\left(-\frac{b_R}{\sqrt{d_R}}+x_R\mathrm{sech}(t\sqrt{d_R}),b_R,d_R\right)\\ &\times\left|\mathrm{sech}(t\sqrt{d_R})\right|\mathrm{d}b_R\,\mathrm{d}d_R. \end{aligned} \quad \text{(A.3)}$$

In both expressions, Eqs. (A.2) and (A.3), $f_{0R}(a_R,b_R,d_R)$ denotes the PDF of the random vector $(a_R(\omega),b_R(\omega),d_R(\omega))^\top$, which can be calculated as the marginal of the PDF of the random input parameters $f_0(a_R,a_C,b_R,b_C,d_R)$. When the RV $d_R(\omega)$ can take both positive and negative values, the 1-PDF can be calculated by the sum of Eqs. (A.2) and (A.3)

$$f_R(x_R,t)=f_R^+(x_R,t)+f_R^-(x_R,t).$$

Now, if $d(\omega)=0$ for all $\omega\in\Omega$, the real contribution of the solution SP is given by $x_R(t,\omega)=a_R(\omega)+b_R(\omega)t$. Then, the 1-PDF is

$$f_1(x_R,t)=\int_{\mathbb{R}} f_{0R}\left(x_R-b_R t,b_R\right)\mathrm{d}b_R,$$

being, in this case, $f_{0R}(a_R,b_R)$ the PDF of the random vector $(a_R(\omega),b_R(\omega))^\top$.

Appendix B. Computing the 1-PDF of the complex component, $x_C(t,\omega)$

In this appendix the 1-PDF of the complex component $x_C(t,\omega)$ is determined. First, we compute the 1-PDF in the first and second scenarios indicated in the introduction, that is, we consider $d_C(\omega)$ a continuous RV. After that, we will assume that the RV $d(\omega)=d_R(\omega)$ has only a real contribution. Finally, we consider that the RV $d(\omega)=0$ for all $\omega\in\Omega$. That is, the coefficient d is zero in the IVP (5).

B.1. Computing the 1-PDF in the first and second scenarios

In this case, the real component $x_C(t,\omega)$ is given in Eq. (9). Let $t>0$ be fixed, we apply the RVT method, Theorem 1, to the mapping $\mathbf{r}:\mathbb{R}^6\to\mathbb{R}^6$

$$\begin{aligned} v_1 &= r_1(\mathbf{u}) = x_C(t) = -a_R g_2(t;\mathbf{y}) + a_C g_1(t;\mathbf{y}) + g_4(t;\mathbf{y}),\\ v_2 &= r_2(\mathbf{u}) = a_C,\\ \hat{\mathbf{v}} &= \hat{\mathbf{r}}(\mathbf{u}) = \mathbf{y}, \end{aligned}$$

where $\hat{\mathbf{v}}=(v_3,v_4,v_5,v_6)$, $\hat{\mathbf{r}}=(r_3,r_4,r_5,r_6)$ and $\mathbf{y}=(b_R,b_C,d_R,d_C)$. The inverse mapping $\mathbf{s}:\mathbb{R}^6\to\mathbb{R}^6$ is

$$\begin{aligned} a_R &= s_1(\mathbf{v}) = \frac{v_2 g_1(t;\hat{\mathbf{v}}) + g_4(t;\hat{\mathbf{v}}) - v_1}{g_2(t;\hat{\mathbf{v}})},\\ a_C &= s_2(\mathbf{v}) = v_2,\\ \mathbf{y} &= \hat{\mathbf{s}}(\mathbf{v}) = \hat{\mathbf{v}}. \end{aligned}$$

The Jacobian of the mapping $\mathbf{s}$ is

$$J=\frac{1}{g_2(t;\hat{\mathbf{v}})}=\frac{1}{-\sin(r_{1C}t)\sinh(r_{1R}t)}=-\frac{\csc(r_{1C}t)}{\sinh(r_{1R}t)},$$

where $r_{1R}=r_{1R}(v_5,v_6)$ and $r_{1C}=r_{1C}(v_5,v_6)$ are the real and complex part of the root $r=\sqrt{d_R+id_C}=\sqrt{v_5+iv_6}$. Then, the PDF of the random vector $\mathbf{v}$ in terms of the PDF of input parameters is

$$f_{\mathbf{v}}(\mathbf{v})=f_0\left(s_1(\mathbf{v}),v_2,\hat{\mathbf{v}}\right)\left|\frac{\csc(r_{1C}t)}{\sinh(r_{1R}t)}\right|.$$

Marginalizing with respect to the random vector $(v_2(\omega),\hat{\mathbf{v}}(\omega))^\top$ and taking $t>0$ arbitrary, the 1-PDF of the complex component of the solution SP of IVP (3)–(4) is

$$\begin{aligned} f_C(x_C,t)=&\int_{\mathbb{R}^5} f_0\left(s_1(x_C,a_C,b_R,b_C,d_R,d_C),a_C,\mathbf{y}\right)\\ &\times\left|\frac{\csc(r_{1C}(d_R,d_C)t)}{\sinh(r_{1R}(d_R,d_C)t)}\right|\mathrm{d}a_C\mathrm{d}\mathbf{y}, \end{aligned} \quad \text{(B.1)}$$

where $\mathbf{y}=(b_R,b_C,d_R,d_C)$.

B.2. Computing the 1-PDF in the third scenario

We compute the 1-PDF in the third scenario, considering that the coefficient of the RDE (3) is a real RV, $d(\omega)=d_R(\omega)$. If $d_R(\omega)$ is a RV with negative domain, the 1-PDF is

$$\begin{aligned} f_C^-(x_C,t)=&\int_{\mathbb{R}^-}\int_{\mathbb{R}} f_{0C}\left(\frac{\sec(\sqrt{-d_R}t)\left(\sqrt{-d_R}x_C-b_C\sin(\sqrt{-d_R}t)\right)}{\sqrt{-d_R}},b_C,d_R\right)\\ &\times\left|\sec(\sqrt{-d_R}t)\right|\mathrm{d}b_C\,\mathrm{d}d_R. \end{aligned} \quad \text{(B.2)}$$

On the other hand, if $\mathbb{P}\left[\omega\in\Omega\,:\,d_R(\omega)>0\right]=1$, the 1-PDF is given by

$$\begin{aligned} f_C^+(x_C,t)=&\int_{\mathbb{R}^+}\int_{\mathbb{R}} f_{0C}\left(-\frac{b_C\tanh(t\sqrt{d_R})}{\sqrt{d_R}}+x_C\mathrm{sech}(t\sqrt{d_R}),b_C,d_R\right)\\ &\times\left|\mathrm{sech}(t\sqrt{d_R})\right|\mathrm{d}b_C\,\mathrm{d}d_R. \end{aligned} \quad \text{(B.3)}$$

In both expressions, Eqs. (B.2) and (B.3), $f_{0C}(a_C, b_C, d_R)$ denotes the PDF of the random vector $(a_C(\omega), b_C(\omega), d_R(\omega))^\top$, which can be calculated as the marginal of the PDF of the random input parameters $f_0(a_R, a_C, b_R, b_C, d_R)$. When, the RV $d_R(\omega)$ can take both positive and negative values, the 1-PDF can be calculated by the sum of Eqs. (B.2) and (B.3)

$$f_C(x_C, t) = f_C^+(x_C, t) + f_C^-(x_C, t).$$

Now, if $d(\omega) = 0$ for all $\omega \in \Omega$, the complex contribution of the solution SP is given by $x_C(t, \omega) = a_C(\omega) + b_C(\omega)t$. Then, the 1-PDF is

$$f_1(x_C, t) = \int_{\mathbb{R}} f_{0C}\left(x_C - b_C\, t, b_C\right) \mathrm{d}b_C,$$

being, in this case, $f_{0C}(a_C, b_C)$ the PDF of the random vector $(a_C(\omega), b_C(\omega))^\top$.

References

[1] B. Goodwine, Engineering differential equations: Theory and applications, Springer, New York, 2011.

[2] M. Tenenbaum, H. Polard, Ordinary Differential Equations: An Elementary Textbook For Students Of Mathematics, Engineering, And The Sciences, Courier Dover Publications, New York, 1985.

[3] W.C. Xie, Differential Equations For Engineers, Cambridge University Press, New York, 2010.

[4] T.C. Gard, Introduction To Stochastic Differential Equations, Marcel Dekker, New York, 1988.

[5] B. Oksendal, Stochastic Differential Equations: An Introduction With Applications, Springer, Berlin, 2007.

[6] T.T. Soong, Random Differential Equations In Science And Engineering, Academic Press, New York, 1973.

[7] J.L Strand, Random ordinary differential equations, J. Differ. Equ. 7 (3) (1970) 538–553, http://dx.doi.org/10.1016/0022-0396(70)90100-2.

[8] T. Neckel, F. Rupp, Random Differential Equations In Scientific Computing, Versita, London, 2013.

[9] M.C. Casabán, J.C. Cortés, J.V. Romero, M.D. Roselló, Solving random homogeneous linear second-order differential equations: A full probabilistic description, Mediterr. J. Math. 13 (2016) 2817–3836, http://dx.doi.org/10.1007/s00009-016-0716-6.

[10] Y. Sibuya, Linear Differential Equations In The Complex Domain: Problems Of Analytic Continuation, vol. 82, American Mathematical Society, Rhode Island, 1990.

[11] E. Hille, Ordinary Differential Equations In Complex Domain, John While & Sons, New York, 1976.

[12] A. Savin, Sternin B., Introduction To Complex Theory Of Differential Equations, Birkhauser Basel, Switzerland, 2017.

[13] A. Joohy, Ordinary Differential Equations In Complex Domain With Applications: In Physics And Engineering, Scholars' Press, Latvia, 2018.

[14] J. Soon-Mo, J. Roh, The linear differential equations with constant complex coefficients and Schrödinguer equations, Appl. Math. Lett. 66 (2017) 23–29, http://dx.doi.org/10.1016/j.aml.2016.11.003.

[15] M.C. Casabán, J.C. Cortés, J.V. Romero, M.D. Roselló, Probabilistic solution of random homogeneous linear second-order difference equations, Appl. Math. Lett. 34 (2) (2014) 27–32, http://dx.doi.org/10.1016/j.aml.2014.03.0102.

[16] J.C. Cortés, A. Navarro-Quiles, J.V. Romero, M.D. Roselló, Solving second-order linear differential equations with random analytic coefficients about ordinary points: A full probabilistic solution by the first probability density function, Appl. Math. Comput. 331 (2018) 33–41, http://dx.doi.org/10.1016/k.amc.2018.02.051.

[17] G. Falsone, D. Settineri, Explicit solutions for the response probability density function of linear systems subjected to random static loads, Probab. Eng. Mech. 33 (2013) 86–94, http://dx.doi.org/10.1016/j.probengmech.2013.03.001.

[18] G. Falsone, R. Laudani, A probability transformation method (PTM) for the dynamic stochastic response of structures with non-Gaussian excitations, Eng. Comput. 35 (2018) 1978–1997, http://dx.doi.org/10.1108/EC-12-2017-0518.

[19] G. Falsone, D. Settineri, On the application of the probability transformation method for the analysis of discretized structures with uncertain properties, Probab. Eng. Mech. 35 (2014) 44–51, http://dx.doi.org/10.1016/j.probengmech.2013.10.001.

[20] R. Laudani, G. Falsone, Use of the probability transformation method in some random mechanic problems, SCE-ASME J. Risk Uncertain. Eng. Syst. A-Civil Eng. 7 (2018) 04020054, 110.1061/AJRUA6.0001111.

[21] J. Eriksson, E. Ollila, V. Koivunen, Statistics for complex random variables revisited, in: Proceedings Of The 34th IEEE International Conference On Acoustics, Speech And Signal Processing, 2009, pp. 3565–3568.

[22] J. Eriksson, E. Ollila, V. Koivunen, Essential statistics and tools for complex random variables, IEEE Trans. Signal Process. 58 (10) (2010) 5400–5408, http://dx.doi.org/10.1109/TSP.2010.2054085.

[23] F.D. Neeser, Proper complex random processes with applications to information theory, IEEE Trans. Inf. Theory 29 (4) (1993) 1293–1302.

[24] A. Khurshid, Z.A. Al-Hemyari, S. Kamal, On complex random variables, Pak. J. Stat. Oper. Res. 8 (3) (2012) 645–654.

[25] S.L. Garrett, The Simple Harmonic Oscillator. In: Understanding Acoustics, Springer, Cham, 2020.

[26] M. Itagaki, S. Suzuki, I. Shitanda, K. Watanabe, Electrochemical impedance and complex capacitance to interpret electrochemical capacitor, Electrochemistry 75 (2007) 649–655, http://dx.doi.org/10.5796/electrochemistry.75.649.

[27] T. Lazimov, On complex inductance in dissipative electrical circuits, Int. J. Adv. Res. Electr. Electron. Instrum. Eng. 5 (2016) 2650–2653, http://dx.doi.org/10.15662/IJAREEIE.2016.0504086.

[28] M. Metropolis, S. Ulam, The Monte Carlo method, J. Am. Stat. Assoc. 44 (1949) 335–341.

[29] C. Proppe, H.J. Pradlwarter, G.I. Schueller, Equivalent linearization and Monte Carlo simulation in stochastic dynamics, Probab. Eng. Mech. 18 (2003) 1–15, 0266-8920(02)00037-1.

[30] D.P. Kroese, T. Taimre, Z.I. Botev, Handbok Of Monte Carlo Methods, Wiley, 2011.